Modelling of Structure-Property Relationship of TMT High Strength Structural Steel Bars

by

ISRAT RUMANA KABIR
Student number: 0411112014

A thesis paper is submitted to the department of Materials and Metallurgical Engineering, BUET in partial fulfillment of the requirements for the degree of Master of Science in Materials and Metallurgical Enginering

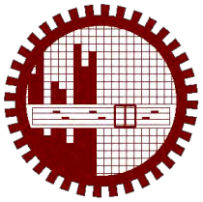

Department of Materials and Metallurgical Engineering
BANGLADESH UNIVERSITY OF ENIGINEERING AND TECHNOLOGY (BUET)
DHAKA-1000, BANGLADESH

June, 2014

DECLARATION

It is hereby declared that this postgraduate thesis, entitled **Modelling of Structure-Property Relationship of TMT High Strength Structural Steel Bars** is accomplished only by me, under the supervision of Dr. Md. Mohar Ali, Professor of the department of Materials and Metallurgical Engineering, BUET, Dhaka. It is also declared that this thesis has not been submitted anywhere for any degree or diploma.

Countersign by Signature

……. ……

Supervisor

Name: **Israt Rumana Kabir**

Student No.: **0411112014**

Dedicated to

My Parents

and

My Respected Faculty Teachers and staffs

The thesis titled **"*Modelling of Structure-Property Relationship of TMT High Strength Structural Steel Bars*"** submitted by **Israt Rumana Kabir**, Student no. : **0411112014**, Session: **April 2011**, has been accepted as satisfactory in partial fulfillment of the requirement for the degree of Master of Science on Materials and Metallurgical Engineering on 17th June, 21014.

BOARD OF EXAMINERS

1. _____

Dr. Md. Mohar Ali — Chairman
Professor — (Supervisor)
Department of Materials and Metallurgical Engineering,
BUET, Dhaka.

2. _____

Dr. Md. Mohar Ali — Member
Professor and Head — (Ex-Officio)
Department of Materials and Metallurgical Engineering,
BUET, Dhaka.

3. _____

Dr. Ahmed Sharif — Member
Associate Professor
Department of Materials and Metallurgical Engineering,
BUET, Dhaka

4. _____

Dr. Kazi Md. Shorowordi — Member
Assistant Professor
Department of Materials and Metallurgical Engineering,
BUET, Dhaka

5. _____

Dr AKM Abdul Hakim — Member
Ex-Director and Chief Engineer, — (External)
Bangladesh Atomic Energy Commission, Dhaka.
231/B Modhobazar, Road 19, West Dhanmondi, Dhaka- 1209.

ACKNOWLEDGEMENT

The author expresses his sincere gratitude and profound indebtedness to Dr. Md. Mohar Ali, Professor and Head, Department of Materials and Metallurgical Engineering BUET, Dhaka, for kind consideration, generosity and whole-hearted supervision, which led me and my thesis work to a successful completion. His experienced outlook in research area, appropriate directions, suggestions and inspirations especially at final stage made this work possible.

I would be grateful enough to thank my former supervisor of this thesis project Dr. Md. Aminul Islam, Professor, Department of Materials and Metallurgical Engineering, BUET, Dhaka, who first believing in me initiates this project. His competence, experience and passion in research have helped me to take confident steps to run experiments. His motivational words, straightforward instructions and kind support regarding this thesis has opened up my analytical power and better perceptions in research.

I would like to extend my best regards to Dr. Fahmida gulshan, Assistant Professor, Department of Materials and Metallurgical Engineering, BUET, Dhaka. Her encouragements always helped me for being persistent and confident towards my work.

I am really grateful to all the professors and teachers of my department for being so well-wisher and well-concern about my accomplishment of thesis to secure a bright future, and cordially helpful to assist my project.

I wish to acknowledge the technical assistance provided by Mr. Md. Harun, Mr. Shamsul Alam Liton, Technicians of Material Testing lab who always helped me to operate machines without hesitation, gave technical and safety knowledge about the machines. I also thank to Mr. Ahmedullah of Metallography lab for always helping, teaching and giving instructions to accomplish the hectic, laborious jobs of Metallography.

I would like to express my thanks and gratitude to all the officials, workers and members/members of Department of Materials and Metallurgical Engineering, BUET, Dhaka, for their kind cooperation and valuable suggestions to complete the thesis on time.

Finally, I would like to extend my sincerity and gratefulness to my parents for their continuous inspirations and supports that encouraged me to complete the thesis successfully.

Above all, all these efforts and attempts would like to deliberately be bestowed towards the almighty Allah who made all this possible.

ABSTRACT

The 500W locally produced thermomechanically treated (TMT) high strength reinforcing steel bars have been collected from four different companies. The chemical compositions of the TMT steel rebars were determined by optical emission spectroscopy (OES) and carbon equivalents (CE) were calculated from the results of the OES. The macro and micro structure of the rebars were studied using metallographic techniques. To determine hardness, Rockwell hardness test and Vickers hardness tests were conducted. Tensile tests were carried out using a Universal Testing Machine (UTM) to evaluate the tensile properties (tensile strength, yield strength, % of elongation) of the rebars in three different conditions viz. with and without rib and without case. The mathematical modelling were developed between the tensile properties (tensile and yield strength) and hardness in the light of previous studies on it. Failure modes of the high strength steel rebars in tensile loading were studied by observing fracture surfaces after tensile tests.

It was found that all TMT steel rebars were low carbon steels having 0.18 percentage of carbon in average. Optical microscopy revealed low carbon martensite in the case and ferrites and pearlites in the core. A transition zone of refined, mixed constituents was also observed in the microstructures. Difference in size, shape and appearance of grains and constituents has been observed. Variations in area of hardened case, core and transition zone of the rebars were revealed in the macrostructures. Differentiation in hardness among the TMT rebars was observed due to the variation in microstructures and chemical compositions. It was also found that the hardness of the cases was higher than that of the cores. The dissimilarity in tensile properties of the TMT steel rebars was found too.

The evaluation of tensile property from the mathematical models was consistent with the tensile properties obtained from the mechanical tensile tests. The yield strength calculated from the strength–hardness models also showed consistency with the test values. The effects of microstructures and carbon equivalent on the hardness and tensile test results were evaluated. Description of the evaluated tensile properties from the mathematical models was also given in terms of the microstructures of the TMT steel rebars. The calculated and test values of tensile properties showed good agreement with the microstructures. The fracture behaviours of the TMT steel rebars also showed good dependency on microstructures. Thus, overall structure-property relationship was established with existing mathematical models.

Table of Contents

List of Figures Page No.

List of Tables Page No.

Chapter 1

INTRODUCTION

Iron and steel industry is one of the major sources for worldwide environmental pollution [1, 2]. As a result, steel producers are in tremendous pressure to produce high strength structural steels so that the annual steel consumption as well as environmental pollution could be reduced. For any structure, there is a relation between the extent of earthquake related damages and overall weight of the structure. So, there is also a growing interest within the reinforced concrete industries in using higher strength reinforcing steel bars for light weight high rise buildings. This interest is driven primarily by the relief of congestion of steel bars in columns or beams, particularly in designing of high earthquake resistant buildings [2-6].

The high strength steel bars can be produced by adding alloying elements in steels like Si, Al, Cr, V, Co, etc. It is also produced subjecting low alloy steels to different kinds of work hardening procedure. But, there are some major kinds of problems arise from these steel strengthening routes. Like as the ductility, formability, bendablity is reduced for increasing strength and hardness. In order to keep off the problems related to inferior ductility, material scientists has been developing for many decades the advanced thermo mechanically treatment to strengthening steels [7-11]. Thermo mechanically treatment might be applied both to plain carbon steels and alloy steels. But, alloy steels may be applied for further higher strength and other required properties as per service conditions [12, 13].

There are different kinds of thermomechanical techniques to strengthen steels with maximum level of ductility, such as quenching and tempering or QT steels, ultrafine grained or UFG steels, dual phase steels, retaining and controlling the proportion of metastable phases, i.e. phases with stress induced transformation behaviour (transformation induced plasticity; TRIP steel), etc. In Bangladesh some steel companies are manufacturing and marketing QT steels as TMT steel [11]. This type of TMT bars are being generally used to reinforce concrete structures in our country. The TMT bars consist of a hard case to strengthen with a soft core rendering ductility. The hard and strong case contains martensitic structures where the soft cores are made of ferrite and pearlite. These combined structures appeared through the special thermomechanical treatment leading to improved tensile properties, high hardness and fatigue resistance [11, 14, 15]. So, all local steel industries of our country is now eagerly driving to manufacture high strength TMT steels by adopting this technology.

In construction applications, tensile properties are very important for design purpose which is usually achieved by destructive tensile tests. Although, it is a very popular test for characterizing tensile behaviours of reinforcing steel bars, this test might have some confusing results. Because, the measured properties are dependent on the geometry, surface condition and other test parameters [16, 17], which are usually not considered in the conventional test methods.

Hardness of the metals implies the resistance to permanent or plastic deformation. It is considered an easy means to measure and quantify as well as good indication about the strength of metals [18]. Ever since the hardness testing has come into existence, it has been using as non-destructive means for quality inspection of metals [19]. There have been many efforts to relate hardness to mechanical properties. Many researchers and scientists have worked on experimental techniques and the theoretical relations to determine strength from hardness over the last century [17, 20-22]. Such relations can be useful in designing, where the direct measurement of tensile properties is not viable [23-24].

In this present study, an initiative has been taken to investigate the tensile and yield strength from hardness and correlate these properties using simple statistical method. The attempt has been done for locally produced thermo mechanically treated high strength steel bars in our country.

The primary motivation behind this present investigation is to compare the conventional tensile strengths of reinforcing steel bars to that obtained by modelling of tensile strengths converted from hardness values of different zones (case and core) of the thermomechanically treated steel bars. Different chemical compositions and surface roughness levels of those steel bars have been used as variants. The effects of microstructures and compositions on the properties have been examined. Finally the fracture behaviors in tensile loading of those steels have been observed and tried to explain in the light of structures.

The results obtained in this project are likely to be useful for understanding the correlation between conventional tensile test results and hardness converted tensile properties. The models possibly help in determining strength from hardness when using small test samples uniaxial tensile test would not be feasible. Small test samples may require during thermomechanical simulations and heat treatment studies or in-situ quality inspection during production in industries. The effects of microstructures and chemical composition on the properties would also be understood from this study. In addition, the effects of process parameters on the properties of the TMT steel bars would be predicted.

The remainder of this report has been divided into some chapters. The second chapter discusses about the literature relevant to this study. The structural steels, the high strength structural steels, the thermo mechanical treatment of producing high strength steels have been discussed in brief in the literature. Besides, the composition, properties and structure of TMT high strength steels, the relation between hardness and strength and the statistical method used for this correlation also have been interpreted. The previous studies and research and their outcomes relating this investigation have been reviewed.

A detail interpretation on Experimental methods and steps has been put in chapter three. The Optical Emission Spectroscopy for determining the chemical compositions, the Metallography techniques to reveal structures of those samples have been explained. The steps of hardness tests and tensile tests have been mentioned in this chapter. The correlation techniques have been also discussed.

Chapter four describes the overall results of all experimentations. The data tables of hardness and tensile tests results, images of microstructures and macrostructures, the graphical presentations of all estimations and the photographs of deformation behaviours have been included in this chapter. The theoretical and logical reasons about the experimental results and observations have been discussed in this chapter.

Finally a conclusion has been drawn from this present attempt and investigations of the structure properties relations of locally produced high strength thermo mechanically treated high strength steel bars. An approach of correlating hardness and tensile properties based on previous studies has been proposed.

The future scopes of this study have been mentioned which is followed by the reference and bibliography of resources used in this study.

Chapter 2

BACKGROUND AND LITERATURE REVIEW

2.1 Structural Steel

Steel has been established for more than 100 years as a construction material and the Eiffel Tower in Paris is a world-wide recognized example demonstrating not only impressively the merits of steel but also its impact on architectural creativity. Probably the most relevant innovation for steel construction within the last century came with the introduction of welding as the major joining technology. Furthermore, the application of high strength steels supported the economics and the elegance of steel as well as reinforced concrete construction. High rise buildings, car park decks, offshore platforms, ocean vessels, bridges, etc. demonstrate the widespread penetration of steel into concrete construction engineering. In civil construction a variety of materials are in competition and this is initiating a continuous technological innovation. This innovation not only concerns the improvement of the materials themselves, but also results in the introduction of new technologies and methods for fabrication, joining and construction [25]. Most steel used for reinforcement is highly ductile in nature. Its usable strength is its yield strength, as this stress condition initiates such a magnitude of deformation (into the plastic yielding range of the steel), that major cracking will occur in the concrete. Since the yield strength of the steel is quite clearly defined and controlled, this establishes a very precise reference in structural investigations. An early design decision is that for the yield strength (specified by the Grade of steel used) that is to be used in the design work [6].

Structural design engineers are looking for high strength and earthquake resistant steel bars for reinforcing concrete to reduce the overall weight of the structures. However, it is really not so straight forward job, because any possible reduction in steel consumption (i.e. overall reduction in structural weight) must be adopted without compromising the safety of the users of buildings and auto bodies. In this situation, application of high strength steel rods/bars/sheets might provide necessary solution. Through the addition of various alloying elements, the strength of steel can be increased. But the key problem concerning this steel strengthening route is that it reduces the ductility of the steel as well as the bendablity or stretch formability. In order to avoid problems related to inferior ductility, materials scientists have developed various advanced structural steels of proper microstructures through precise control of various thermomechanical treatments‘ parameters. Thermomechanically treated steels

might be plain carbon as well as alloy steels. The latter group of steels (alloy steels) are designed to achieve further higher strength along with other property requirements depending on service conditions [11].

It is to be noted that there are various technological options to increase the strength of structural plain carbon steels such as by increasing carbon content, addition of other alloying elements, decreasing ferrite/pearlite grain size, changing ferrite/Pearlite structure to high strength bainitic structure by water spray/sudden cooling, proper cleaning of molten steels, thermo-mechanical treatment and so on [11]. Here in this paper, initiative will be taken to discuss techniques to increase the strength of steels by various thermomechanical treatments with their possible advantages. There are various thermomechanical treatment techniques such as quenching and tempering (QT, note: in Bangladesh some steel companies are marketing this type of product as TMT steel), severe refining of the grain size of steels (ultrafine grained; UFG steel), controlling the soft and hard phases of the steels (e.g. dual phase; DP steel), retaining and controlling the proportion of unstable/metastable phases, i.e. phases with stress induced transformation behaviour (transformation induced plasticity; TRIP steel), etc.

2.2 Thermo mechanically Treated (TMT) High strength steel bars

This group of structural steel might be plain carbon or alloy type. In general, it is bar type product used for reinforcement of concrete. However, it can also be used for load bearing machine components or other structural applications. In the case of conventional bars, the hot rolled products are cooled naturally in the air. So, from surface to core, the microstructures remain fully ferrite-pearlite. But for QT/TMT steel bars, they are forced to cool suddenly by passing them through water chamber just after final rolling. So, the outer layer of the bar gets quenched with subsequent formation of tempered martensite at the outer layer. The structures of the core remain as normal ferrite-pearlite and there is also a transition zone exists in between the outer tempered martensite and ferrite pearlite core (Fig.2.1). Tempered martensite is a very strong phase, which provides high strength and relatively soft ferrite-pearlite structure at core provides necessary ductility of the steel.

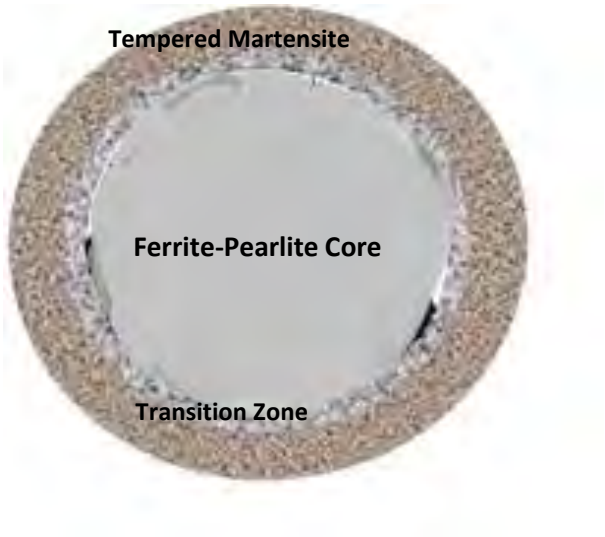

Fig.2.1: The structure of the QT/TMT steel with Tempered Martensite Case, Ferrite-Pearlite Core and Transition Zone middle of the Case and Core [11].

2.2.1 Chemical Composition

Thermo mechanically treated or TMT deformed steel bars are high strength steel bars for reinforcing concrete structures. The TMT is a metallurgical process that integrates work hardening and heat-treatment into a single process. The process quenches the surface layer of the bar, which pressurizes and deforms the crystal structure of intermediate layers, and simultaneously begins to temper the quenched layers using the heat from the bar's core [26]. This quenching and work hardening processes give rise to high strength steel bars from the low carbon steels. In Bangladesh, TMT grade-500W (weldable) has been produced for some years. All local companies are following international specifications for choosing billets of specified chemical compositions to produce TMT high strength steel rebars. A specified table of chemical composition for some TMT steel bars and other grades has been mentioned as follows.

Table 2.1: Practiced Standard chemical compositions of TMT grade and 60 grade steels [26].

Steel Type *	Chemical Compositions						
	C	Si	Mn	S	P	Cr	Cu
PC-TMT	0.18	0.4	0.74	0.03	0.02	-	-
Cu-TMT	0.2	0.4	0.7	0.03	0.03	-	0.2
Cu-Cr-TMT	0.2	0.4	0.7	0.03	0.03	0.2	0.2
ASTM A706 Grade 60	o.3max	0.5max	1.5max	0.045	0.04	-	-
Typical Alloy 60 Grade in Bangladesh	o.32	0.4	1.2	0.045	0.04	0.1	0.2

* PC= Plain Carbon

2.2.2 Structure:

Generally the hot-rolled deformed steel bars are produced from the mild steel. Mild steels are low carbon steels which lie in the hypoeutectoid steel area of the Iron-Iron Carbide phase diagram. The microstructures of hypoeutectoid are normally consisted of ferrite phase and pearlite. As TMT steel bars undergo a distinct process of production consisting deformation followed by the heat treatment like quenching and tempering of surface layer of the bars, the structures, both micro and macro, of these TMT steel bars are unlike to the conventional deformed steel bars.

2.2.2.1 Macrostructure

When the cut ends of TMT bars are etched in Nital (a mixture of nitric acid and methanol), three distinct rings appear: 1. a dark grey outer ring called case, 2. a inner circular zone of light grey colour called core and 3. an annular ring of whitish grey colour in between the case and core named transition zone. This is the desired macro structure for quality construction rebars (Fig. 2.2) [14, 27].

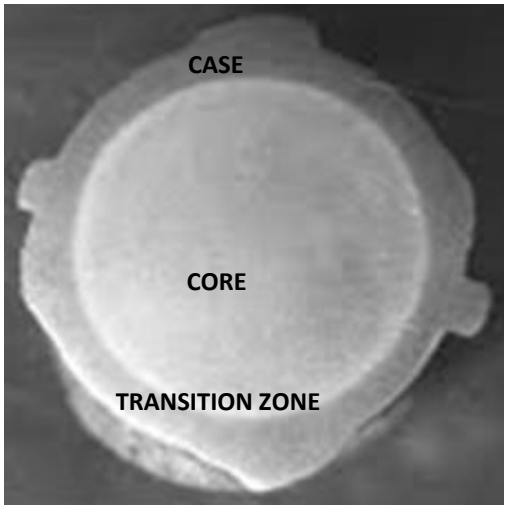

Figure 2.2: Macrostructure of the cross section of TMT steel rebar [27].

2.2.2.2 Microstructure

These bars therefore exhibit a variation in microstructure in their cross section. The Case has strong, tough, tempered low carbon martensite in the surface layer of the bar. The transition zone is an intermediate middle layer of martensite and bainite, and finally the core is made of a refined, tough and ductile ferrite and pearlite (Fig. 2.3) [14, 27].

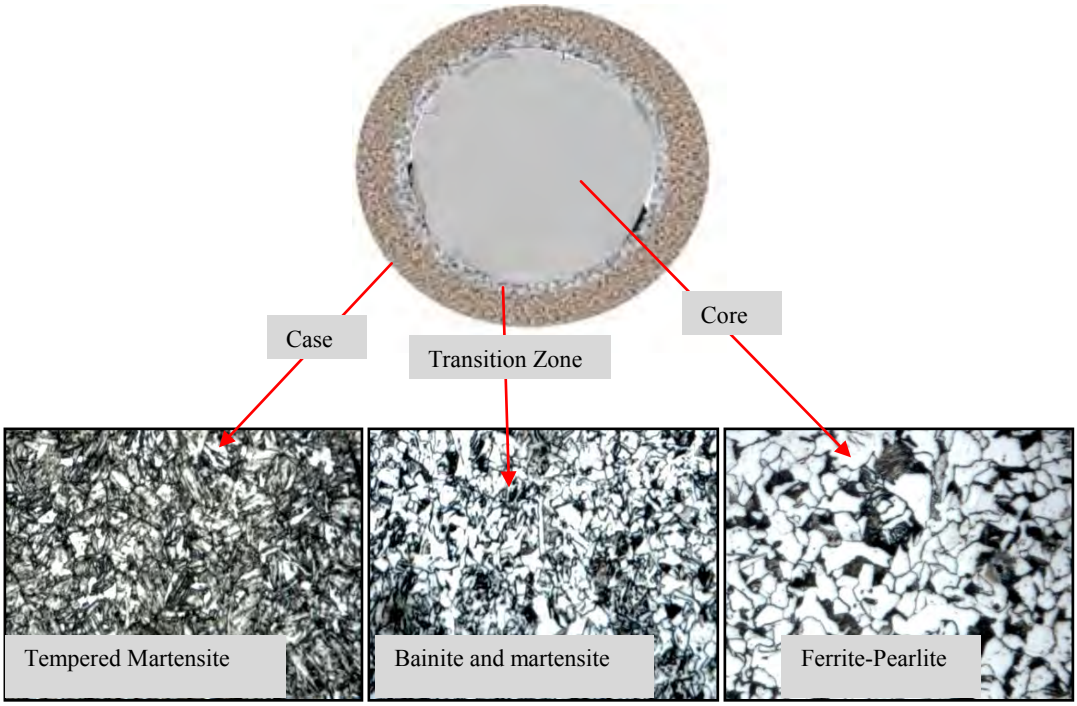

Figure 2.3: Microstructures of different zones of TMT steel bar [27].

2.2.3 Mechanical Properties

The thermo mechanical technology of manufacturing steel bars adopts a wide range of mechanical properties in the low carbon steel rebars. The quenching process of surface layer of the bar gives a hard strong wear resistance surface. Additionally, the soft ferrite-pearlite core renders ductility and toughness. The hardness and corrosion resistance of this steel bar are also better than the conventional steel bars. So, a lot of properties are accommodated in low carbon steel reinforcing bars through this technology. Some properties have been listed below [28-30].

a. Higher yield strength
b. Higher toughness
c. Higher resistance to brittle cleavage
d. Higher resistance to low-energy ductile fractures
e. Good ductility and bendablity
f. Improved hardness and wear resistance.

2.2.3.1 Tensile Properties

Tensile properties are important characteristic indication for reinforcing steel bars in designing safe, strong, sustainable structures. The TMT high strength steel rebars exert better tensile properties than conventional rebar. We get a combination of good YS, TS and ductility. Though conventional low carbon rebars show higher ductility, lower strength but in case of thermomechanically treated low carbon rebars, a good combination of higher strength and good ductility can be attained. Such good combination of strength and ductility is very effective to reinforcing bars in structural application. The well combined microstructures of TMT bars render good combination of tensile properties. The hard case, of tempered martensite gives high yield and tensile strength and toughness. The softer core of ferrite-pearlite contributes to good ductility. A schematic stress-strain curve has been shown in figure 2.4 [11].

The 500W grade produced in our country, show minimum 500 MPa YS and TS of upto 575 MPa with minimum 14% of elongation [31].

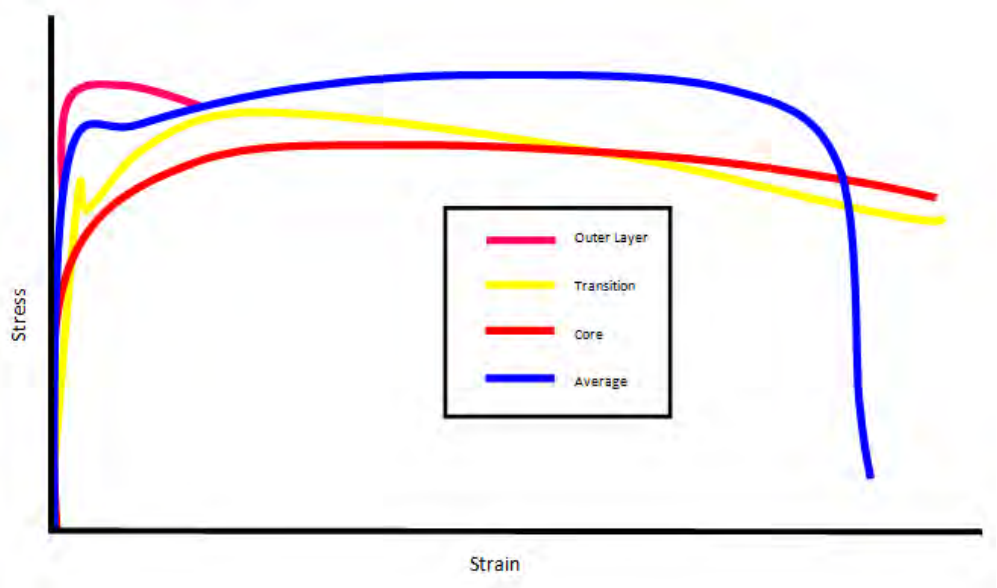

Figure 2.4: Schematic representation of stress-strain curve exerts from different zones of TMT rebar [11].

2.2.3.2 Hardness

Hardness is another important characteristic of selecting good steel for reinforcing concrete. Hardness like strength defines the resistance against deformation plastically of the material. It is very easy to measure and is a very popular non-destructive test for quality inspection of materials. The hardness of

TMT bars is greater than the conventional hot rolled bars because of the tempered martensite and other strong phases present in its microstructure. Generally martensite exerts upto 60 HRC depending on the percentage of carbon present in steel [32].

2.2.3.3 Parameters regulate the mechanical properties of steels:

The size of the grain, or average grain diameter, in a polycrystalline metal influences the mechanical properties. A fine-grained material is harder and stronger than one that is coarse-grained material. For many materials, the yield strength, σ_y, varies with grain size according to the Hall-Patch equation, where d is the average gain diameter, and σ_0 and k_y are constant for a particular material.

$$\sigma_y = \sigma_0 + k_y d^{-1/2} \qquad (2.1)$$

Grain size may be regulated by the rate of solidification from the liquid phase, and also by plastic deformation followed by an appropriate heat-treatment. It should be mentioned that grain size reduction improves not only strength but also the toughness of many alloys [33].

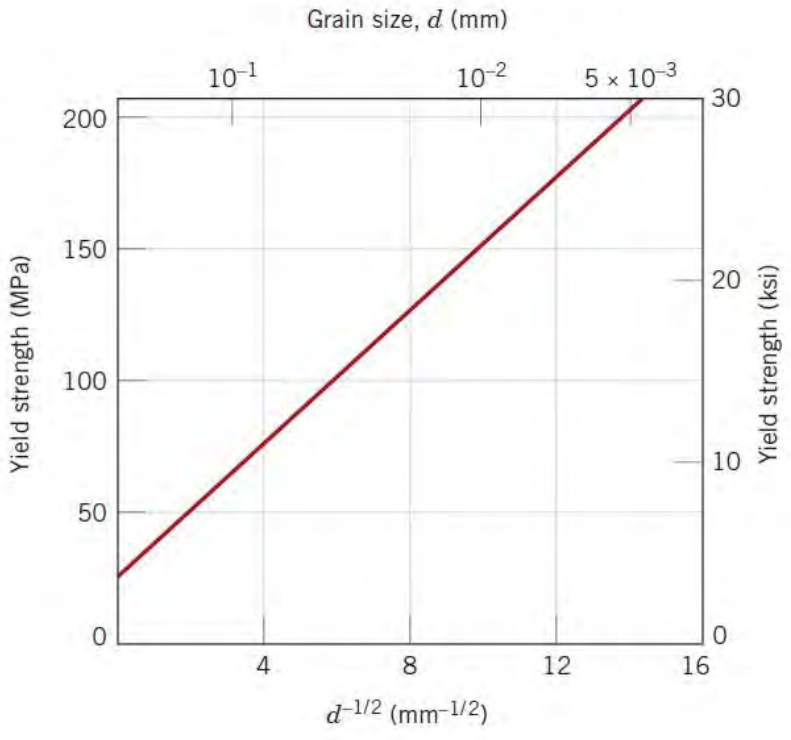

Figure 2.5: The influence of grain size on the yield strength [33].

2.2.4 Heat Treatment of TMT High strength steel bars

TMT high strength steel bars undergo in-situ heat treatment process during rolling. After the last pass of deformation from the rolling strand, in thermo mechanical process, the steel rebars are passed through a quenching box for some seconds. In the quenching box, a cool water flow is sprayed over the surface of the hot rolled rebars. The temperature before entering this box should be above of the upper critical temperature of steels. As a result the surface of the rebars gets quenched and the austenite grains of surface layer turn to martensite and it shrinks. This shrinkage pressurizes the core and helps to form correct crystal structures. The core yet remains hot and austenitic. A temperature gradient develops across the cross-section of the rebars. After leaving from the quenching box, an auto tempering occurs of the rebars due to the temperature gradient between the surface and the core (Fig. 2.8). The temperature of the core conducts to the surface and it starts to cool slowly. The cooling converts the austenite of the core to ferrite and pearlite. The conducted heat from the core tempers the martensite of the surface and eventually causes a hard, strong case of tempered martensite. A transition zone appears in the middle of the case and core of mixed structures of some martensite, bainite and small grains of ferrite-pearlite of different shapes. Thus an automatic tempering process is created through the thermo-mechanically technique [28]. A schematic view of quenching box and the temperature difference causes the formation of case and core has been shown in Fig. 2.6.

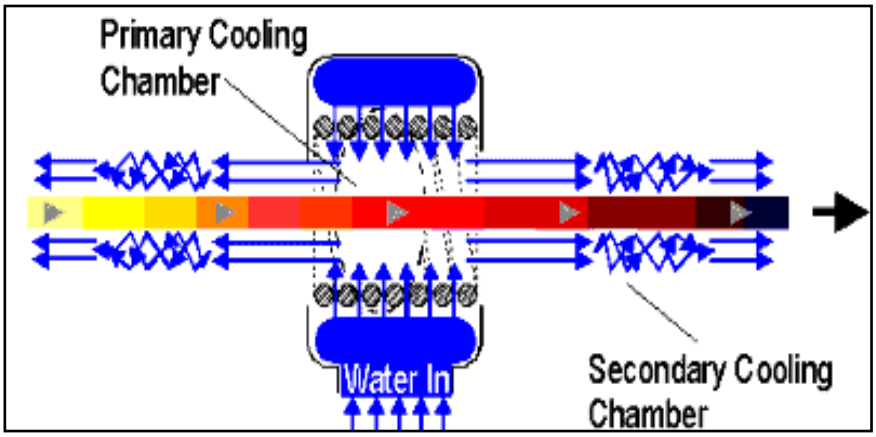

Figure 2.6: Schematic diagram of quenching box used for TMT steel bar production [27].

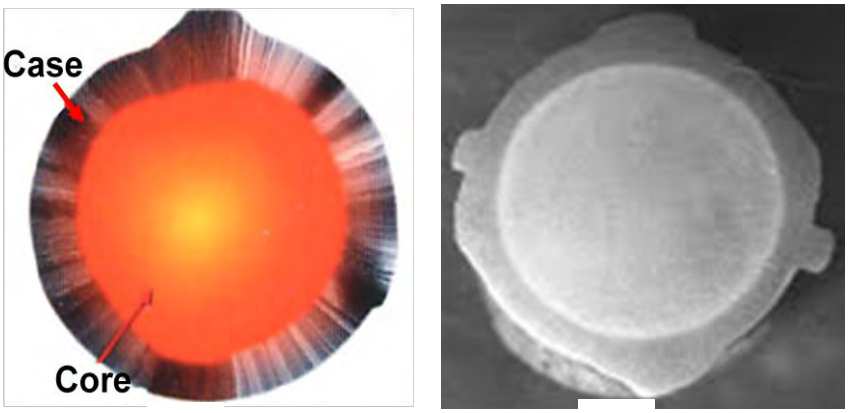

Figure 2.7: Cross-section of TMT steel bar just after (a) water quenching and (b) after final cooling [27].

2.2.4 Effect of alloying elements on the structure and properties of TMT

The effects of elements on the structure and properties on TMT steel bars as same as other types of steel. The primary elements of steel like Carbon, Manganese, Silicon, Phosphorous and Sulfur have the similar effects. The other secondary elements those are generally used for alloying steels like Copper, Chromium, Nickel, Vanadium, etc. have the effects on corrosion resistance, strengthening steels and increasing hardness and wear resistance. But in TMT process of producing reinforcing steel bars, those secondary elements are not intentionally added in a significant amount. During production of billets, these elements come into the melts as trump element from different sources. But, these elements usually help to enhance properties of the TMT bars to some extent [14].

Table 2.2 shows the influence of different chemical ingredients of steel on the properties of rebar. Characterization is generally performed by checking the chemical composition and certain specified physical properties. The particular chemical ingredients and physical properties, which are selected for characterization, again depend on the attributes of the material that are important for its specified application [14].

Table 2.2: Influence of different chemical ingredients in steel on properties of rebars [14].

No	Chemicals	Controlling property	Actual effect
1	Carbon (C)	Hardness, strength, weldability and brittleness	Higher carbon contributes to the tensile strength of steel, that is, higher load bearing capacity and vice versa. Lower carbon content less than 0.1 percent will reduce the strength. Higher carbon content of 0.3 percent and above makes the steel bar unweldable and brittle.
2	Manganese (Mn)	Strength and yield strength	Higher manganese content in steel increases the tensile strength and also the carbon equivalent property.
3	Sulphur (S)	Present as an impurity in steel which increases its brittleness.	Presence of higher sulphur makes the bar brittle during twisting, as higher sulphur content brings the hot shot problem during rolling.
4	Phosphorus (P)	4 Present as an impurity which increases strength and brittleness	Higher phosphorus content contributes to the increase in strength and corrosion resistance properties but brings brittleness due to the formation of low euctoid phosphicles in the grain boundary. Also lowers the impact value at sub zero temperature level (transition temperature).
5	Copper (Cu)	Strength and Corrosion Resistance properties	Being a pearlite stabilizer, it increases the strength and corrosion resistance property.
6	Chromium (Cr)	Weldability and Corrosion resistance	Present as an impurity from the scrap and influences carbon equivalent; weldability and increases corrosion resistance property.
7	Carbon Equivalent (CE or C eq)	Hardness, tensile strength and weldability	This property is required to set the cooling parameters in TMT process and a slight variation in carbon equivalent may alter the physical properties.

2.2.5 Residual Stress in TMT Bar

Thermo-mechanical process is a combined process of hot-rolling and heat treatment. The deformation due to hot-rolling and the quenching heat treatment process of the TMT steel rebars both develop an internal stress inside the rebars. This internal stress is called the residual stress occurs in TMT rebars. The internal stress occurred due to hot rolling is kind of uniform and compressive type stress in rebars [1]. Additionally, the quenching of surface of rebars causing martensitic transformation of the austenite grains of surface of the rebars also create internal stress onto the core [28, 29]. These residual stresses due to deformation and quenching process retain if the standard heat treatment schedule of the TMT steel rebars does not properly be maintained. A standard heat treatment schedule of TMT bar manufacturing process is given by Fig. 2.8 [3, 4]. This kinds of residual stress can increase strength and hardness resulting develop brittleness of TMT rebars.

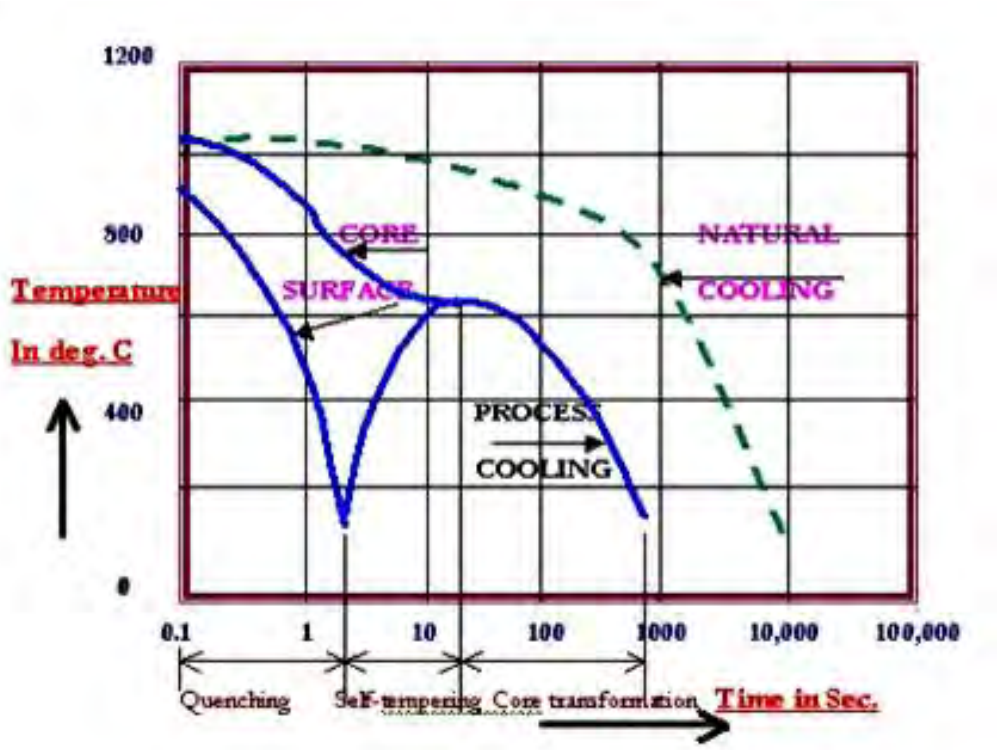

Figure 2.8: Diagram showing the standard heat treatment schedule for TMT steel bar production [3, 4, 27].

2.2.6 Effect of hardened zone on properties of TMT

The hardened zone of the TMT rebars is the case. As the surface layer of the TMT rebars undergone a quenching process and consequently got martensitic structure, this martensite is a metastable phase get itself tempered due to the flow of heat energy from the core and transformed into ferrite and carbide. This tempered martensitic layer is hard, strong and brittle in nature. This layer contributes in increasing strength and hardness of the TMT rebars. Due to the tetragonal martensite increases the volume of the cubic austenite grains after transformation, it also causes internal stress into the rebars. The dislocation density increases due to martensitic transformation [1]. Notch sensitivity increases. But the soft ductile core compensates the hardness with toughness and ductility to the rebars. The corrosion resistance increase due to the surface refined low carbon martensite grains.

2.3 Correlation of Hardness with Tensile Strength and Yield Strength

Both tensile strength and hardness is indicator of a metal‘s resistance to plastic deformation. Consequently, they are roughly proportional to tensile strength as a function of the brinell hardness of cast iron, steel and brass. The same proportionality relationship does not hold for all metals, as indicating in Fig. 2.9. As a rule of thumb for most steel, the HB and the tensile strength are related according to

$$TS(MPa) = 3.45 * HB \quad (2.2)$$

$$TS(psi) = 500 * HB \quad (2.3)$$

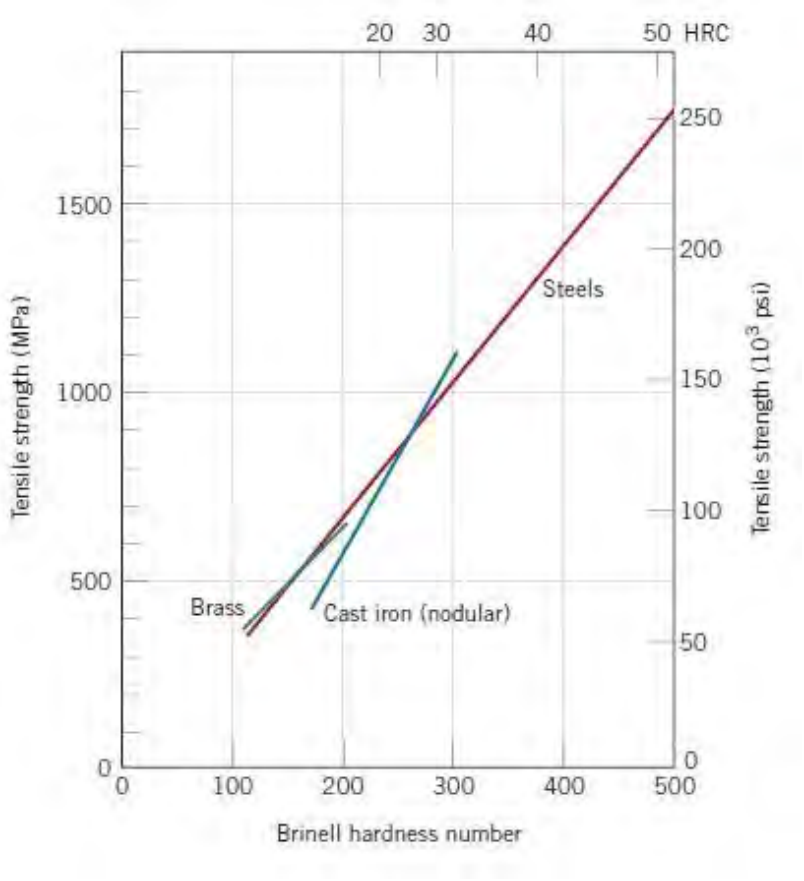

Fig 2.9: Relationship between hardness and tensile strength for steel, brass, and cast iron [33].

2.3.1 Previous studies:

Many researchers have been working on the correlation of hardness with strength of metals from the last century. Initially, a very useful engineering correlation between Brinell hardness and the ultimate

tensile strength of heat-treated plain carbon and medium alloy steels was proposed. This relation was for spherical indentation [34],

$$\text{UTS (psi)} = 500\ (\text{BHN}) \tag{2.3}$$

This showed a good agreement with the Tabor's results. Tabor made a simplifying assumption for a class of material which does not strain harden, where UTS is equal to the yield strength. The equation is

$$\sigma_u = 1/2.8 * p_m \tag{2.4}$$

where p_m is the Meyer hardness in kg/mm2. Upon converting this equation with engineering units and Brinell hardness gives rise to [34]

$$\sigma_u = 515\ (\text{BHN}) \tag{2.5}$$

Tabor worked on various types of indentation and hardness tests to correlate that resultant hardness with strength of various types of steels, alloys and metals [35, 36]. He shown for Diamond pyramid hardness the ultimate tensile strength of a material is given by,

$$\sigma_u = (H/C)(1\text{-}n)\ \{12.5/(1\text{-}n)\}n \tag{2.6}$$

where H, Diamond pyramid hardness or Vickers hardness, n is the strain hardening co-efficient, and C is the constant which has a value 2.9 for the steels and 3.0 for copper [21, 35, 36]. It has been shown theoretically and confirmed experimentally that [37],

$$n = m\text{-}2 \tag{2.7}$$

where m is the meyer's hardness co-efficient, also the true stress- strain curve in the plastic region can be approximated by

$$\sigma = k\epsilon n, \tag{2.8}$$

where ϵ is the true strain and k is the constant. Tabor used those eqs. (2.7), (2.8) and the additional information, H/2.9 which is approximately equivalent to the stress at a strain of 8% during tensile test of steels, and derived [38],

$$\sigma_u = (H/2.9)\,[1-(m-2)]\,[12.5*(m-2)/\,1-(m-2)](m-2) \qquad (2.9)$$

However, there appeared to have been no attempts to obtain a general expression relating the 0.2% offset yield strength yet of metals to hardness. Atkins and Tabor derived compressive stress-strain curves for steels and copper from hardness measurements but could not extend the curve below 4% strain. A good correlation between the 0.2% offset yield strength and hardness for many different steels in the quenched and tempered condition has been established [38] but the reasons for the correlation were not investigated, nor was the treatment extended for other metals. It was shown [39] that the yield strength of a severely cold worked material should be given by

$$\sigma_y = H/3 \qquad (2.10)$$

this relation has been verified experimentally to some degree, but for this derivation it is assumed that the strain hardening has not occurred. However, Marcinkowski et al. [40] showed for annealed Fe-Cr alloys which exhibited some strain hardening that $a_y \sim H/5$. Speich and Warlimont [41] found that $a_y \sim H/4$ for some low carbon martensites and Fe-Ni alloys.

Cahoon et al. [21, 36, 42, 43] offered expressions relating hardness and tensile strength and yield strength in the form of

$$TS = (H/2.9)\,(n/0.217)n \qquad (2.11)$$

and

$$YS = (H/3)\,(0.1)n \qquad (2.12)$$

Where TS and YS are tensile strength and yield strength respectively, and n is the strain-hardening exponent. These expressions show excellent agreement (<2%) in calculating the tensile properties of a ferritic steel at temperatures up to 4000 C (Ref 7). Use of Cahoon‘s expressions requires prior knowledge of the strain-hardening exponent either directly from uniaxial tensile tests or indirectly through Meyer‘s index or empirical methods [21, 23].

Pavlina and Van Tyne [21, 43] suggested simple linear relationships to estimate the ultimate tensile strength and yield strength using the Vickers hardness number for steels as follows:

$$YS = -90.7 + 2.876\,Hv \qquad (2.13)$$

$$UTS = -99.8 + 3.734\ Hv \quad (2.14)$$

where strength has units of MPa and Hv has units of kg/mm^2. These relationships do not require the knowledge of any other parameter than hardness for estimation of strength.

The Vickers hardness Hv can be related to various flow stresses of materials σ by the following equations

$$Hv = A\sigma \quad (2.15)$$

where A is a constant[19, 39, 44-46]. Here the flow stress and hardness are usually given in MPa. Theoretical analysis based on two-dimensional slip lines indicates that the values of the constant A are around 2.9-3.1 [44]. In the analysis, the materials were assumed to be ideally plastic; thus the effect of work hardening was neglected.

Douthwaite and Petch [45] reported that for mild steels the proportionality constant of the hardness to tensile strength σT is ~3. In the Metals Handbook [19], proportionality constants (to σ_T) of 2.8-3.2 for carbon and alloy steels in the annealed, normalized, and quenched and tempered conditions are recommended, varying from high strength to low strength. Slavskii and Artemev [46] suggested a proportionality constant of 3.62 to 0.2% yield stress σ_Y for steels with a broad range of strengths.

In an attempt to predict tensile properties from a hardness test, Lai and Lim [20, 24] found that the strain hardening co-efficient n and the strength coefficient K were linearly related to the hardnesses of steels with various structures. Applying the derived equations to calculate σ_T and σ_Y,

$$\sigma_T = K(100\ Fn)n / \exp(n) \quad (2.16)$$

$$\sigma_Y = K[K(\sigma 0/E + 0.2)n / E + 0.2]n \quad (2.17)$$

where F is a constant less than unity and is dependent upon the material, and E is Young‘s modulus. A good agreement has been obtained between the calculated and experimental results.

More recently, the M. Umemoto et al. [20] suggested that the proportionality constant A_Y relating hardness to yield strength depends strongly on the microstructure of steels for values in the range 3.17-5.79. It is highest for ferrite steel and lowest for martensitic steel. This difference can be attributed mostly to the effect of work hardening behaviour resulting from different structures. They also proposed that, the structural dependence of the proportionality constant A_T relating hardness to

tensile strength was found to be less significant than that of A_Y. The relationship between hardness and yield stress is well represented by the equation proposed by Cahoon et al. [36] taking $\epsilon_y = 0.004$.

2.4 Statistical Modelling

A statistical model is a formalization of relationships between variables in the form of mathematical equations. A statistical model describes how one or more random variables are related to one or more other variables. The model is statistical as the variables are not deterministically but stochastically related. In mathematical terms, a statistical model is frequently thought of as a pair (Y, P) where Y is the set of possible observations and P the set of possible probability distributions on Y. It is assumed that there is a distinct element of P which generates the observed data. Statistical inference enables us to make statements about which element(s) of this set are likely to be the true one.

Most statistical tests can be described in the form of a statistical model. For example, the Student's t-test for comparing the means of two groups can be formulated as seeing if an estimated parameter in the model is different from 0. Another similarity between tests and models is that there are assumptions involved. Error is assumed to be normally distributed in most models [47]

Statistical formulations or analyses which, when applied to data and found to fit the data, are used to verify the assumptions and parameters used in the analysis. Some examples of statistical models include the linear model, binomial model, polynomial model, and two-parameter model [48]

2.4.1 Regression Analysis Tool

In statistics, regression analysis is a statistical process for estimating the relationships among variables. It includes many techniques for modeling and analyzing several variables, when the focus is on the relationship between a dependent variable and one or more independent variables. More specifically, regression analysis helps one understand how the typical value of the dependent variable (or 'criterion variable') changes when any one of the independent variables is varied, while the other independent variables are held fixed. Most commonly, regression analysis estimates the conditional expectation of the dependent variable given the independent variables – that is, the average value of the dependent variable when the independent variables are fixed. Less commonly, the focus is on a quantile, or other location parameter of the conditional distribution of the dependent variable given the independent variables. In all cases, the estimation target is a function of the independent variables called the regression function. In regression analysis, it is also of interest to characterize the variation

of the dependent variable around the regression function which can be described by a probability distribution.

Regression analysis is widely used for prediction and forecasting, where its use has substantial overlap with the field of machine learning. Regression analysis is also used to understand which among the independent variables are related to the dependent variable, and to explore the forms of these relationships [49]

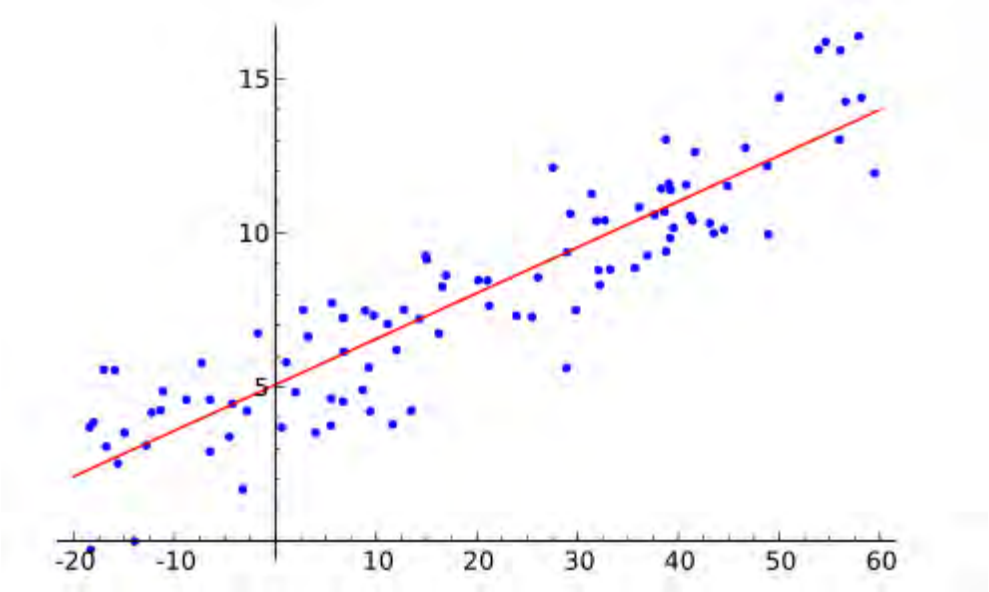

Figure 2.10: A representative linear regression plot [50].

2.5 Law of mixture theory

In materials science, a general rule of mixtures is a weighed mean used to predict various properties of a composite material made up of continuous and unidirectional fibers [51-54]. It provides a theoretical upper- and lower-bound on properties such as the elastic modulus, mass density, ultimate tensile strength, thermal conductivity, and electrical conductivity [54]. In general there are two models, one for axial loading (Voigt model) [53, 55], and one for transverse loading (Reuss model) [53, 56].

In general, for some material property E (often the elastic modulus [52]), the rule of mixtures states that the overall property in the direction parallel to the fibers may be as high as

$$E_c = f.E_f + (1\text{-}f)\, E_m \qquad (2.18)$$

Where

$$f = \frac{V_f}{V_f + V_m}$$

$f = \{V_f\} / \{V_f + V_m\}$ is the volume fraction of the fibers

E_f is the material property of the fibers

E_m is the material property of the matrix

Chapter 3

EXPERIMENTAL PROCEDURES

This chapter contains the interpretation of the detailed procedures followed by the experimentations of the thermo-mechanically treated steel reinforcing bars (rebars) that have been undergone to fulfil the objectives of this research.

3.1 MATERIALS SELECTION

The materials used in this experiment were locally produced TMT high strength steel bars of 20 millimetres diameter from four different companies. They were bought from the local market. These high strength steel reinforcing bars have been popular and demandable for few years in the constructional and structural engineering in Bangladesh.

3.2 EXPERIMENTAL PROCEDURE

3.2.1 Optical Emission Spectroscopy (OES)

The chemical compositions of the collected steel bars of four different re-rolling steel factories were analysed by Optical Emission Spectroscopy (OES) technique. A Shimadzu PDA- 7000 OES machine was used to serve this purpose. For this experiment, samples were cut in cross-section from the stock materials of about 2.5 cm along the length. Three samples for each group of steel rebars were taken. The faces of cross-sectioned samples were firstly ground in a grinding wheel. After that, two faces of each sample were polished with emery papers to create smooth flat faces without any tilting surface for the OES. Total six sparks were taken in both faces for each group and the average data were considered as the representative chemical compositions of the steel bars.

3.2.2 Metallography:

In order to reveal the different zones, to measure the depth of the hardened zones, and to know the microstructures, metallography was performed of the TMT steel rebars. Metallography is a very important for characterising materials. Metallography reveals microstructures of the samples, and it is the microstructure which directly governs all kinds of properties and performances of materials in service. For this experiment metallographic samples need to be prepared.

3.2.2.1 Sample preparation:

Metallographic samples were also cut in cross-section from the stock materials of about 2.5 cm along the length. The faces of cross-sectioned samples were ground in a grinding wheel. Then, these faces were subjected to progressive dry polishing with a series of emery papers of different grit size (from 150 -1200 emery paper no. consecutively) following the standard procedure. After that, wet polishing was done in rotating clothe wheel at 400 rpm with gamma alumina powder (powder size 0.05 μm) and water. When the faces were free from all scratches and became flat and smooth, the samples were washed in water and dried with acetone. These samples were then ready to be etched. Etching is the procedure in Metallography which reveals the right structure by using the right etching solution. We used 2% Nital solution (2% HNO_3 acid in Ethanol) as etching reagent for these steel rebars.

3.2.2.2 Identification of different kind of zones:

After etching the different zones of these TMT steel rebars were revealed. Different zones were observed in naked eyes and were photographed by digital camera.

3.2.2.3 Measurement the depth of hardened zone (Case):

With the help of optical microscope and rular, the case depths and thus case areas were calculated. At first, the images of macrostructure of the steel samples were taken by camera fitted in microscope. Then with help of a ruler, the depth of outer annular ring (case) was measured from minimum 20 places from the images. After that, the average depth was accounted as the case depth of the samples. The hardened zone (case) and unaffected soft zone (core) are shown in the following Figure 3.1.

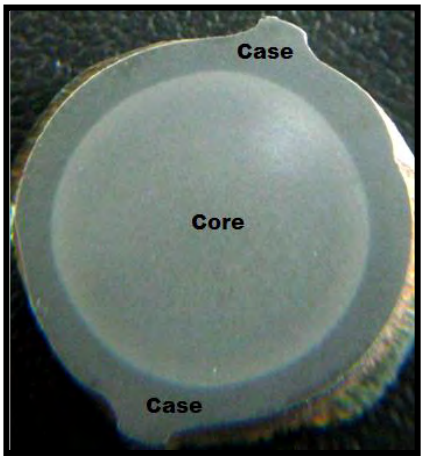

Figure 3.1: Different zones revealed after etching of the TMT rebar.

3.2.2.4 Microstructure analysis:

The microstructures were observed under the optical microscope (Olympus BH2) at different magnifications. The structures of different zones were photographed by digital camera fitted with the microscope at the magnification of 500x and 200x, which processed the image with the help of Leica DC View software.

The microstructures at different zones of the high strength steel bars were also observed under optical microscope and they were photographed.

3.2.3 Rockwell Hardness Test:

After clearly identifying the core and case areas, series of hardness measurements were carried on individual zones. In this case we used Rockwell hardness tester named Future-Tech, FR- 1E. The case areas were harder and core areas were relatively softer. So, case hardness was measured in Rockwell C scale (RHC) and the hardness at core areas was measured in Rockwell B scale (RHB). Square shaped indenter that is Brale penetrator was used for measuring hardness of the cases in Rockwell C scale and the weight applied was 150 kg. To measure the hardness of the soft core region in Rockwell B scale, a spherical steel ball indenter of 1/16 inch diameter was used and the load of 100 kg was applied.

3.2.3.1 Case Hardness:

A series of indents were taken along the periphery of the case area with sufficient distance of interval to avoid strain hardening effects of deformation. The series of hardness values of the case were averaged and presented the hardness of the case in HRC scale. This procedure was repeated for each sample of the groups.

3.2.3.2 Core Hardness:

Similarly, for the circular core region, a series of indentations along the diameters from different directions, after the annular case area, were taken. These series of hardness data were also averaged and presented as HRB hardness of the core.

In this study, the hardness of the transition zone was not considered separately. It was included in the core hardness data.

3.2.3.3 Graphical representations of hardness data:

Simple graphical plots of hardness data corresponding to case and core were prepared using microsoft excel. These graphs show the deviation and similarity of hardness value along the periphery of the annular case and along the diameters of the core.

3.2.4 Conversion of Hardness values into Tensile Strength:

The hardness values thus obtained were converted into tensile strengths following standard chart. The ASTM A370-68 [57, 58] standard chart which expresses approximate relationship between hardness number and tensile strength was followed.

For individual hardness values of both case and core the converted tensile strength was plotted as a function of hardness in Excel to develop a mathematical relationship between the hardness and tensile strength for both case and core areas. This was done individually for both steels. At last, resultant tensile strengths of the steel bars were calculated using the following Eq. 3.1 [16].

$$UTS = \%Case\ area \times Case\ Strength + \%Core\ area \times Core\ Strength \quad (3.1)$$

Finally, relationships between structure and tensile property were developed and they were compared with the conventional tensile strength values of both steel bars.

3.2.5 Vickers Hardness Test:

The polished samples which clearly revealed the core and case areas after etching have been taken to measure Vickers hardness number. Series of hardness measurements were carried out on individual zones. In this case we used Digital Vickers hardness tester of Future-Tech Company, Model no. FV-800. The diamond pyramid shaped indenter was used for measuring Vickers hardness. The test load was applied was 5kgf and dwell time for applying load was 15 seconds.

Case

A series of indents was taken along the periphery of the case area with sufficient distance of interval, to avoid strain hardening effects of deformation. This series of hardness value of the case was averaged and presented the hardness of the case in Vickers scale. This procedure was repeated for each sample of the groups.

Core

Similarly, for the circular core region, a series of indentations along the diameters from different directions, after the annular case area, was taken. These series of hardness data was also averaged and presented as Vickers hardness of the Core.

In this study, the hardness of the transition zone was not considered separately. It was included in the core hardness data.

3.2.6 Tensile Test:

To know the mechanical behaviours of the steel bars, conventional tensile tests were carried out. A Universal tensile testing machine of Shimadzu of UH-500KNA capacity was used to accomplish this experiment. From these tests, yield strengths, ultimate tensile strength and percentage of elongations were recorded. Here it is to be mentioned that tensile tests were carried for samples of two different surface conditions; namely with and without rib to understand the effect of surface conditions and presence of rib on the tensile fracture mode. Tensile samples used in this investigation are shown in Figure 3.2.

Figure 3.2: The samples of steel rebars prepared for the tensile test (a) removing ribs from the surface and (b) the keeping ribs on surface.

3.2.6.1 Observation of fracture mode:

The gross fracture modes of each kind of samples after the tensile test were observed and photographed by digital camera.

3.2.6.2 Determining the ratio of tensile strength to yield strength:

The ratio of tensile strength to yield strength determined from the mechanical tests has been calculated/used. For case the tensile to yield strength ratio obtained from the tensile tests result of the

steels without rib (leaving the case and core) has been used. And for core that TS/YS ratio which was obtained from the tests result of those steels without case (keeping core behind) has been used.

3.2.7 Correlation with hardness and Yield strength:

Unlike the tensile strength, the yield strength cannot be converted from the standard conversion chart. In this study, we followed two methods to determine yield strength from the experimental hardness values of the steels. All the calculations have been done for both Case and Core of the steels separately.

3.2.7.1: Correlation using the TS/US ratio:

In first method, the ratio of tensile strength to yield strength determined from the mechanical tests has been calculated/used. For case the tensile to yield strength ratio obtained from the tensile tests result of the steels without rib (leaving the case and core) has been used. And for core that TS/YS ratio which was obtained from the tests result of those steels without case (keeping core behind) has been used. Now, the converted tensile strength has been converted to yield strength using the ratio. The tensile strengths were converted from the Rockwell hardness values of the steels by following the ASTM standard chart of conversion. This converted yield strength with its corresponding values of Rockwell hardness has been plotted. From this plot a linear regression equation has been determined correlating the hardness and yield strength. This procedure has been executed for all four types of steel and for their case and core separately. Again, resultant yield strength of the steel bars were calculated by using the following equation [16].

$$YS = \%Case\ area \times Case\ YS\ Strength + \%Core\ area \times Core\ YS\ Strength \quad (3.2)$$

Finally, relationships between structure and tensile property were developed and they were compared with the conventional tensile strength values of both steel bars.

3.2.7.2: Correlation from empirical equations:

E. J. Pavlina and C. J. Van Tyne [43] suggested simple linear relationships to estimate the ultimate tensile strength and yield strength using the Vickers hardness number for steels. They correlate the

yield strength to Vickers hardness according to the variations of microstructures. They divided the microstructures of steels into three categories: (1) martensitic microstructures, which include as-quenched and quenched and tempered martensite, (2) non-martensitic microstructures, which include ferrite/pearlite, bainite, and acicular ferrite, and (3) complex phase microstructures, which are those that consist of mixtures of ferrite and other phases such as bainite, martensite, or retained austenite. Two regression equations correlating the Vickers hardness to yield strength for the microstructures of martensitic steels and non-martensitic steels were used in this study. Those equations are mentioned below.

$$YS = 110.9 + 2.507\,Hv, \text{ for martensitic structures} \quad (3.3)\ [43]$$

$$YS = -84.8 + 2.646\,Hv, \text{ for non-martensitic structures} \quad (3.4)\ [43]$$

where, YS refers the yield strength of the steels and H_V indicates the Vickers hardness number.
Now, all Vickers hardness data for case and core of the steel rebars obtained from the test has been put into the Eq. 3.3 and Eq. 3.4 respectively. Yield strengths were calculated for both case and core. Then, the average yield strengths of case and core were put into the Eq. 3.2 and calculated the total yield strength for the steel rebars.

Chapter 4

RESULT AND DISCUSSION

4.1 Chemical Composition:

The chemical compositions of the TMT high strength steel bars are presented in Table 4.1. From this table, it is clear that the chemical compositions of the steel bars are slightly differed from each other. In order to know the combined effect of the alloying elements of the steel bars, their carbon equivalent (CE) values were also calculated using a widely used Eq. 4.1 in line with other investigators [59, 60]. The CE values thus obtained are also presented in Table 4.1.

$$CE = \%C + \left(\frac{\%Mn + \%Si}{6}\right) + \left(\frac{\%Cr + \%Mo + \%V}{5}\right) + \left(\frac{\%Cu + \%Ni}{15}\right) \quad (4.1)$$

From Table 4.1, it is revealed that the percentage of Carbon (C) and Manganese (Mn) for TMT steels is lower than that of conventional 60-grade steels (Table 2.1). With the increase of C and Mn contents strength increases in steels [12]. But, for TMT high strength steel, strength is increased through work hardening and heat treatment techniques rather than increase of C. Here, C content is remained low to increase steel‘s weldablity. Steel 2 and 4 show similar CE values, but those have different percentage of carbon content. The rest Steel 1 and 3 have different CE values from each other. The phosphorus (P) and sulphur (S) contents are lower for all steels. Steel 1 has higher copper (Cu) content than others which play role in increasing corrosion resistance [12, 13].

Table 4.1: Chemical compositions of the reinforcing steel bars (20mm) obtained from OES.

Name of Groups	C	Si	Mn	S	P	Cu	Cr	Ni	CE
Steel 1	0.16	0.14	0.7	0.01	0.01	0.24	0.07	0.07	0.33
Steel 2	0.16	0.20	0.8	0.01	0.01	0.18	0.04	0.05	0.35
Steel 3	0.18	0.17	0.8	0.002	0.003	0.08	0.06	0.03	0.36
Steel 4	0.18	0.20	0.7	0.01	0.01	0.10	0.03	0.03	0.34

The C contents of steel 1 and steel 2 are same that is 0.16 percent. Similarly, steel 3 and steel 4 both have 0.18 percent carbon. Silicon (Si) content is greater in steel 2 and steel 4 of valuing 0.20%. Steel 1 has the lowest Si content that is 0.14%. Steel 3 possesses 0.17% of Si which is slightly higher than steel 1 but lower than steel 2.

The maximum Mn content is 0.8 observed in both steel 2 and steel 3. Steel 1 and steel 4 both have 0.7 % of Mn which is slightly lower than other steels. Steel 3 has the lowest S and P contents which are 0.002% and 0.003% respectively. Rest three steels have same amount of S and P counted 0.1 percent. The maximum Cu content is 0.24% seen in Steel 1 and the minimum content of Cu has been counted in steel 3 of about 0.08 percent. Steel 1 and steel 3 have greater amount of chromium (Cr) than others of nearly same values. Steel 2 and steel 4 show Cr contents of very near amount that are 0.4 and 0.3 percent respectively. The carbon equivalents (CE) of the steels are 0.33, 0.35, 0.36, and 0.35 in order of steel ID given in table 4.1.

4.2 Metallography:

The Metallography to find out the structures for the TMT steel bars has been divided into two courses. One is Macroscopy and other is Microscopy. The structures of the steel rebars have been observed under Light Optical Microscope (LOM).

4.2.1 Optical Macroscopy:

The optical microscopy has been done to reveal the discrete zones appeared in the TMT steel rebars due to heat treatments. To do that the polished and etched samples have been observed and photographed under the LOM in small magnification so that whole cross area has been covered.

4.2.1.1 Determination of Case Depth and the area fractions of Case and Core of the bars:

After polishing followed by etching metallographic sample of each TMT steels show three different zones. One is dark grey coloured outer annular zone called case. Second zone is transition zone next to the case area, a narrow annular zone, of whitish grey colour. The third zone is next to transition zone, a circular zone of light grey colour, called the core. Following photographs presented all these three zones for each steel type.

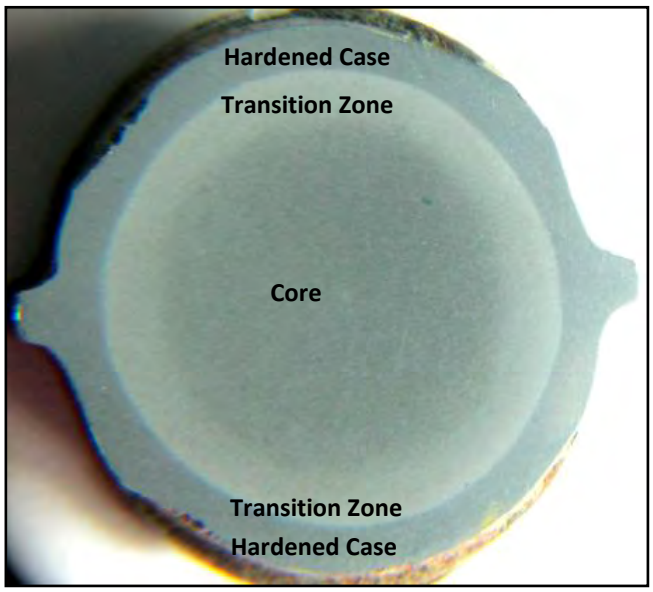

Figure 4.1: Macrograph of the cross section referring outer hardened case, middle transition zone and inner softer core of steel 1 (M. 3x).

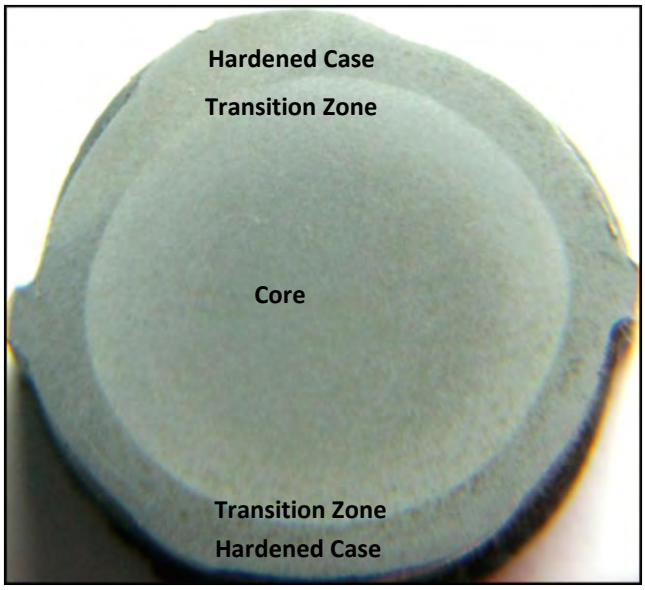

Figure 4.2: Macrograph of the cross section referring outer hardened case, middle transition zone and inner softer core of steel 2 (M. 3x).

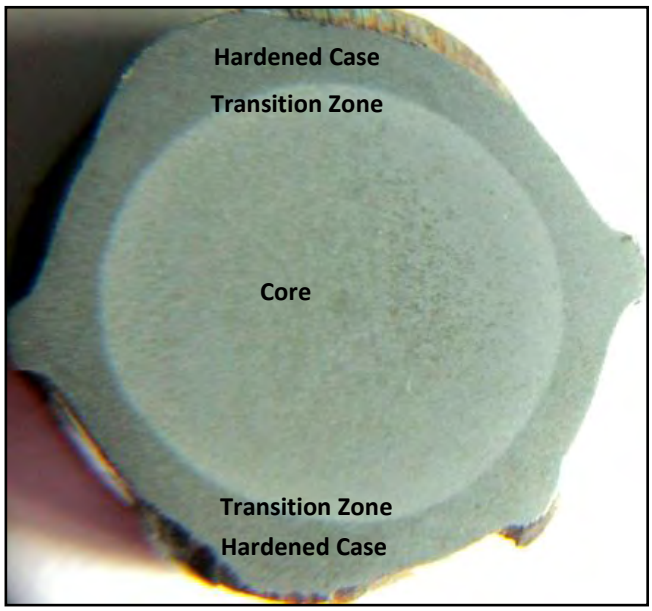

Figure 4.3: Macrograph of the cross section referring outer hardened case, middle transition zone and inner softer core of steel 3 (M. 3x).

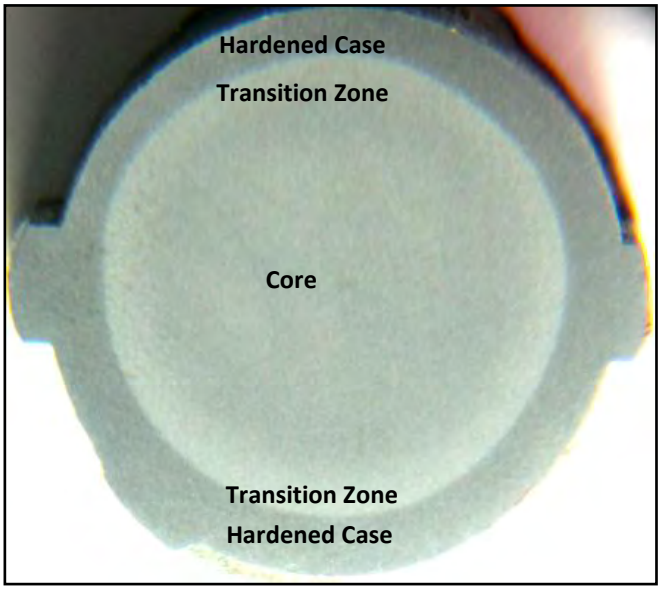

Figure 4.4: Macrograph of the cross section referring outer hardened case, middle transition zone and inner softer core of steel 4 (M. 3x).

Fig. 4.1 shows the three different zones of steel 1. It is clear from this figure that, the case depth of steel 1 is not uniform. The rib width of steel 1 is smaller and rib height is greater than other three types of steel rebars. The transition zone of steel 1 is wider than the rest three kind of steel rebars.

The core area is clearly observed with a distinct circular boundary. Fig. 4.2 presents the case, core and transition zones of the steel 2. The case depth of steel 2 is seemed slightly greater than the steel 1. The transition zone of steel 2 is narrower than steel 1 and the core area is not clearly separated from the transition zone. Steel 2 has the smallest rib height among these four types of steel rebar. Three zones of steel 3 are delineated in Fig. 4.3. Steel 3 has a uniform case with the narrowest transition zone next to case. The core area is separated by a less visible boundary after the transition zone. The rib height of steel 3 is greater than steel 2 and 4 but rib width is more or less similar like steel 1. Steel 4 also shows its three zones in Fig. 4.4. The case area of steel 4 is almost uniform. It has the widest rib but height is small. The core area has quite clear boundary next to the transition zone. But the annular transition zone is not uniform along the periphery.

The case depth has been measured of these steel rebars with a micrometer fitted microscope. To know the case depth of the hardened zone of the TMT steel bars, case depths from different places are measured and their average is considered as the representative value. The average case depths, fractions of case and core areas in terms of the total cross sectional area are given in Table 4.2.

Table 4.2: Case depth and area fraction of case and core of steel rebars.

Steel ID	Case Depth, mm	% Area of Case	% Area of Core
1	1.80	33	67
2	2.00	36	64
3	2.10	38	62
4	1.95	35	65

From Table 4.2, it is clear that case depths of steels are different. The highest case depth is measured in the steel 3. On the other hand, the case depths followed an ascending order with respect to steel 1, 4 and 2. The dissimilarities for case depths have been observed, although all steel bars were followed similar production modules. But, in practice, the production parameters, especially rolling schedule and cooling rates may make this variation. This will also be visually clear from the macrographs of the cross sections of the steel bars shown in Figs. 4.1 to 4.4.

4.2.2 Optical Microscopy:

The polished samples of steels were etched to observe their microstructures under the optical microscope in large magnification. Microstructures of three different zones (case, core and transition zone) of each type of steel were observed. The following figures present those structures of different steel bars.

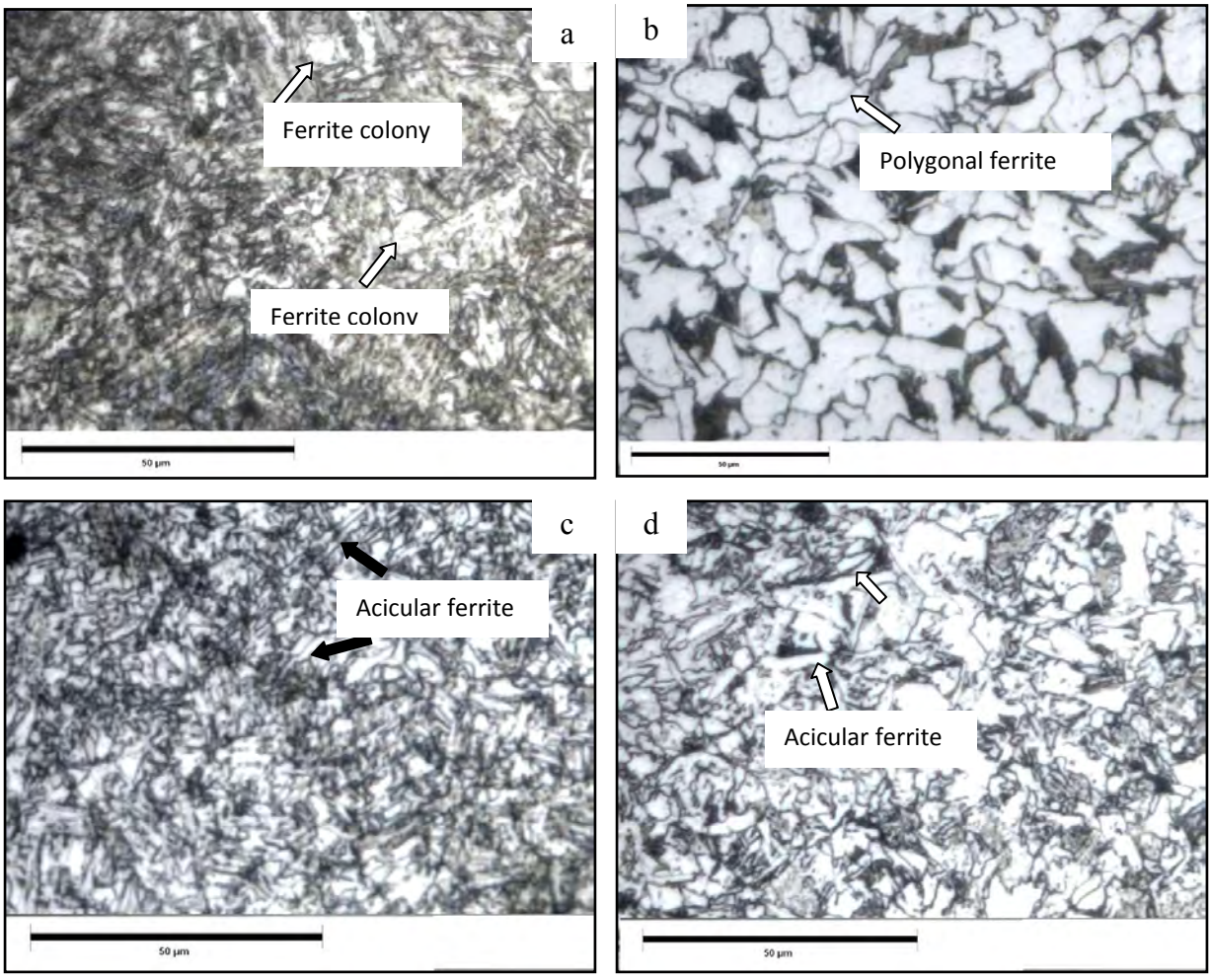

Figure 4.5: Microstructures of steel 1 showing, (a) Case contains Tempered Martensite, Ferrite colony , (b) Core contains Polygonal ferrite, pearlite, (c) Transition zone adjacent to the case having Tempered martensite, bainite, polygonal ferrite, acicular ferrite, and (d) Transition zone adjacent to the core consists of Polygonal ferrite, acicular ferrite, fine pearlite, bainite. (Magnification 50x)

Fig. 4.5 depicts the microstructures of three zones of steel 1. The case of steel 1 is composed of tempered low carbon martensite, some bainite, and a few of ferrite colony delineated in Fig. 4.5 (a). The core structure consists of equiaxed (white) ferrite grain and pearlite (black), which is shown in figure 4.5 (b). Fig. 4.5 (c) and (d) show the microstructures of transition zone adjacent to case and core respectively. Transition zone adjacent to case composed of small acicular ferrite and some amount of bainite and tempered martensite. Bainite cannot be identified by optical microscopy. However, some bainite must be remain in transition zone which can be justified through cooling curve and I-T (Isothermal Transformation) diagram of the low carbon TMT steel bars. But, in Fig. 4.5 (d) the transition zone near the core composed of polygonal ferrite, acicular ferrite (arrow) with a few of small pearlite grains and bainite.

Fig. 4.6 presents the microstructures of three different zones of steel 2. From Fig. 4.6 (a), it is seen that the case of steel 2 is composed of low carbon tempered martensite, bainite, and some ferrite colony like steel 1. The core structure shown in Fig. 4.6 (b) also consists of equiaxed (white) ferrite grain, acicular ferrite and pearlite (black) like steel 1. But, the percentage of pearlite is seemed greater than steel 1 in the core structure, although steel 1 and steel 2 have both similar percentage of carbon. Fig. 4.6 (c) and (d) expressed the microstructures of transition zone of steel 2 adjacent to case and core respectively. Transition zone (TZ) adjacent to case composed of small acicular ferrite and some amount of bainite, martensites. But the transition zone near the core composed of polygonal ferrite, acicular ferrite with a few of small pearlite grains.

Fig. 4.7 (a), (b), and (c) represent the case, core and transition zone of steel 3 respectively. From the chemical composition of Table 4.1, it is seen that the carbon percentage of steel 3 is greater than steels 1 and 2. The case consists of similar type of low carbon tempered martensite, bainite and ferrite colony. Unlike the steels 1 and 2, steel 3 has refined core structure. Fig. 4.7 (b) depicts that, the core composed with some refined polygonal ferrites, some refined acicular ferrites and some pearlite grains, and the transition zone (Fig. 4.7c) is somehow similar with core, consisting of a lot of acicular ferrite grain and pearlite and a few amount of bainite.

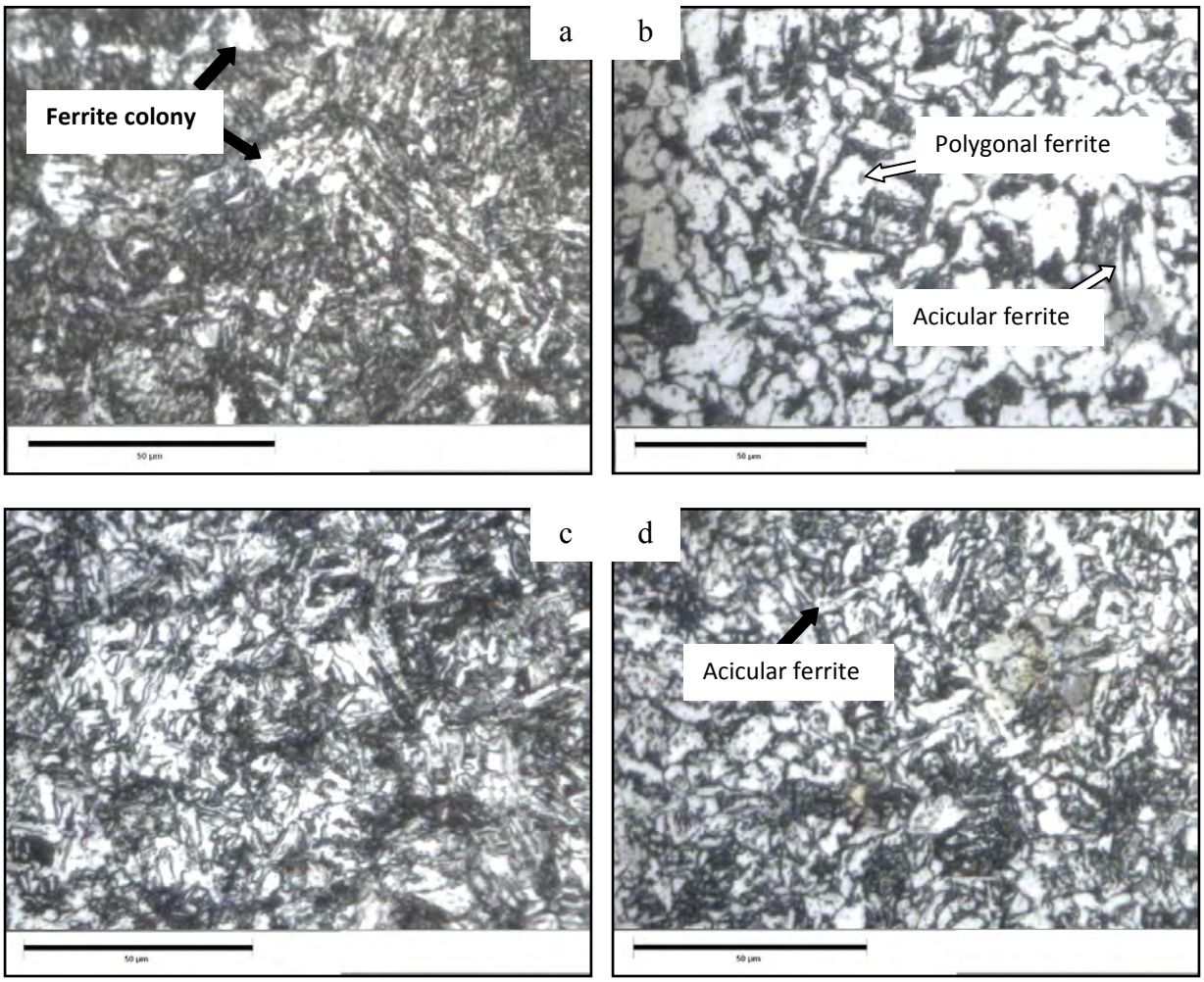

Figure 4.6: Microstructures of steel 2 showing (a) Case having Tempered martensite, ferrite colony , (b) Core contains Polygonal ferrite, acicular ferrite , pearlite, (c) Transition zone adjacent to the case consists of polygonal/acicular ferrites, tempered martensite, bainite, and (d) Transition zone adjacent to the core having polygonal ferrite, acicular ferrite , bainite. (magnification 50x)

The microstructures of three zones of steel 4 are shown in Fig. 4.8 (a), (b), and (c). The carbon percentage of steel 4 is same with steel 3. The case structure again composes with low carbon tempered martensite, bainite and ferrite colony like formers. The core of steel 4 shown in Fig. 4.8 (b) is quite different from other steels. The grains of pearlite and equiaxed ferrites of steel 4 are larger than the steels 1, 2 and 3. There are also some acicular ferrite grains in the core. The transition zone of steel 4 consists of acicular ferrite grain, pearlite and a few amount of bainite shown in Fig. 4.8 (c).

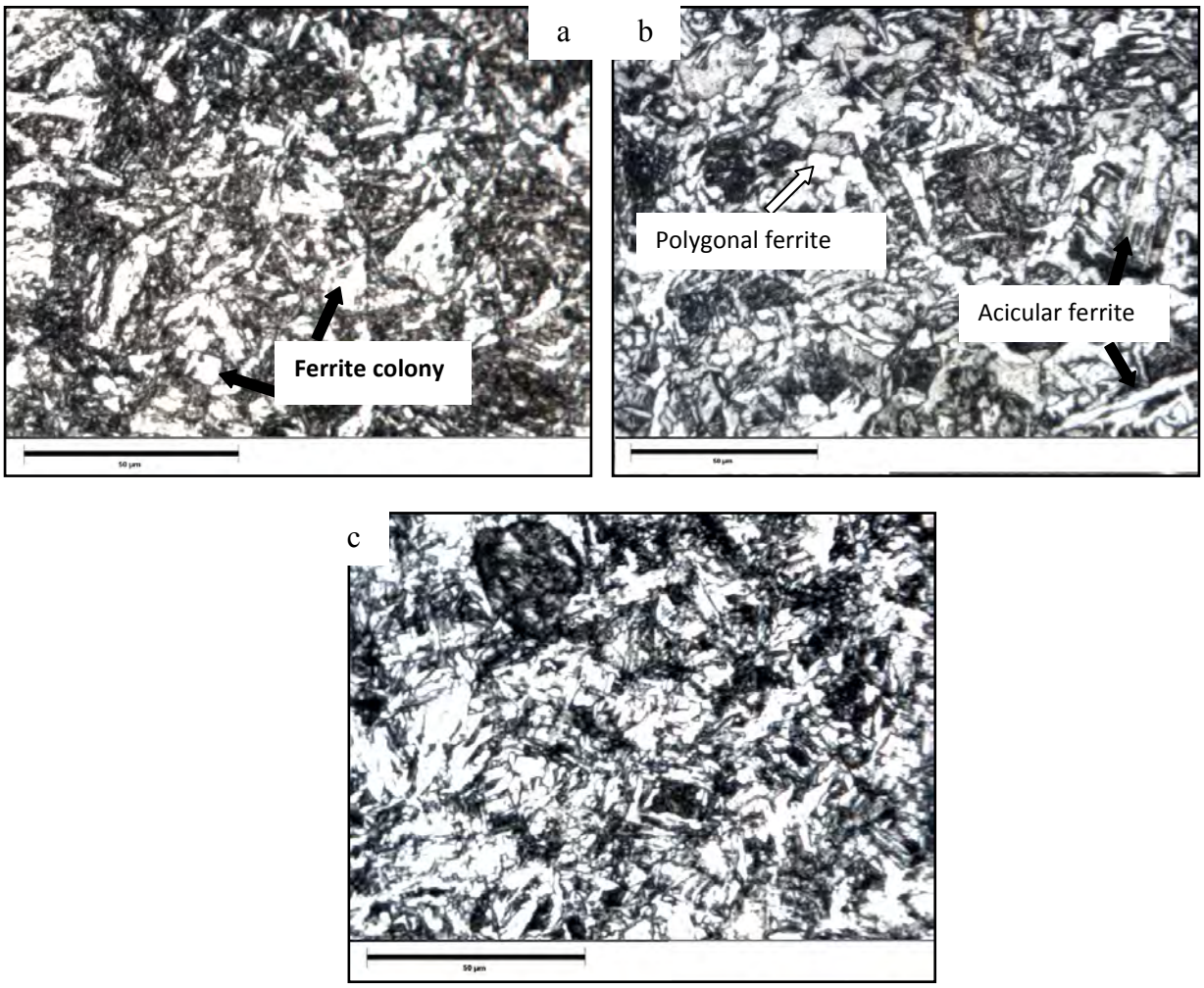

Figure 4.7: Microstructures of steel 3 showing (a) Case contains tempered martensite, ferrite colony, (b) Core made of refined polygonal ferrite, acicular ferrite, pearlite, (c) Transition zone having polygonal ferrite , acicular ferrite , bainite, fine pearlite. (magnification 50x)

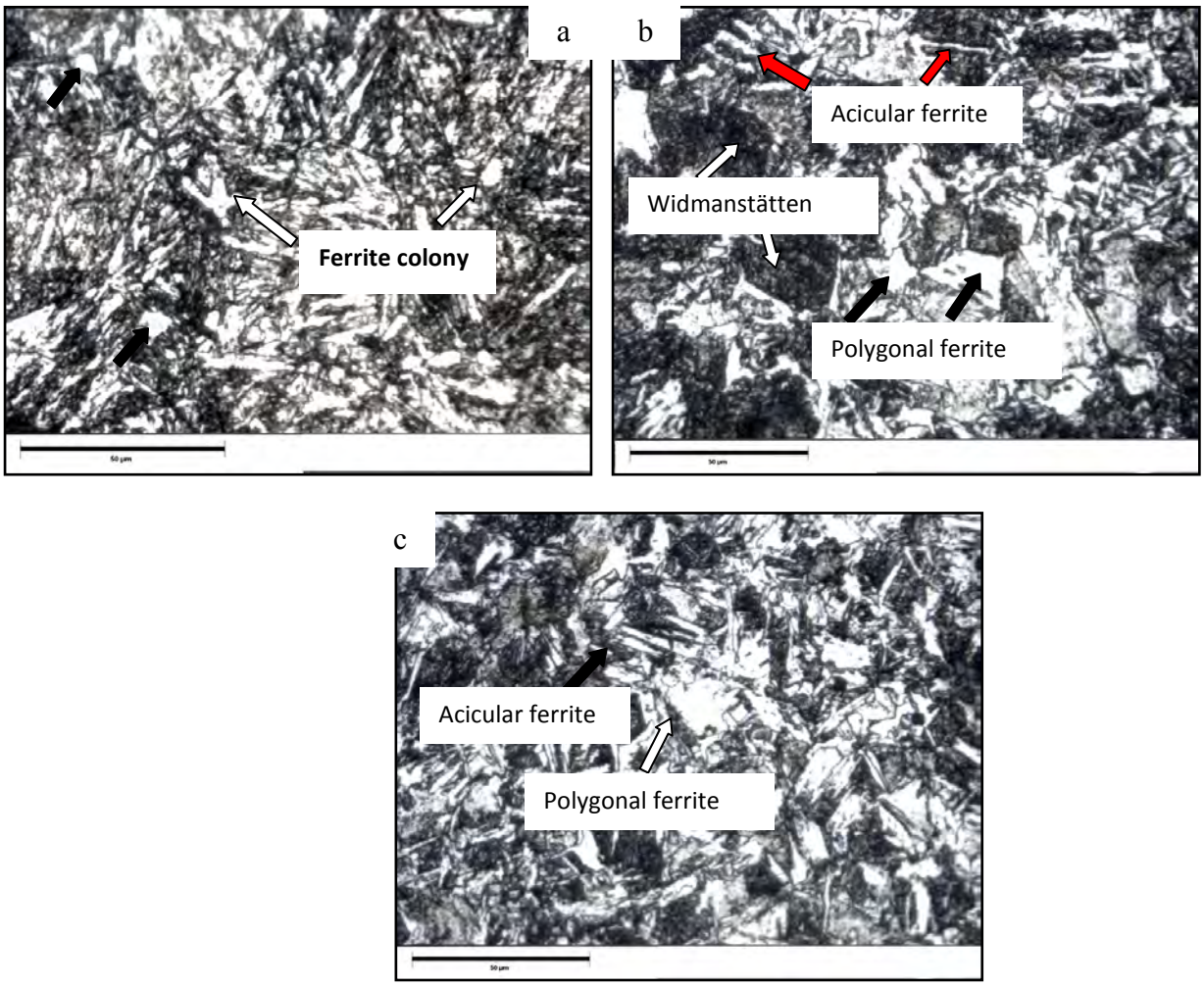

Figure 4.8: Microstructures of steel 4 showing (a) Case having tempered martensite, ferrite colony, (b) Core made of polygonal ferrite, acicular ferrite, pearlite, Widmanstätten structures, and (c) Transition zone contains polygonal ferrite , acicular ferrite, bainite. (magnification 50 x)

4.2.2.1 Comparative study of microstructures of case and core:

From the Fig. 4.5b and Fig. 4.6b it is clear that, the percentage of ferrite is greater in steel 1 than steel 2. And the percentage of pearlite is greater in steel 2 than steel 3. If the grain size of the ferrite and pearlite is considered, then, the Figs. 4.5b and 4.6b show that steel 2 has smaller grains for ferrite and pearlite but steel 1 has larger grains of ferrite and pearlite. Though, steel 2 contains some large grains of ferrite and pearlite along with the small grains. The shape of all ferrite grains in steel 1 almost polygonal or equiaxed, but the ferrite grains in steel 2 are seemed in mixed shape. Steel 2 has shown different shaped ferrite grains with some large and small polygonal grains of ferrite.

The strength of a material increases with the reducing the grain size, increasing the carbon content, adding alloying elements and increasing the percentage of pearlite and hard phases. From the table of composition, it has been shown that, the percentage of carbon is similar for steel 1 and 2. These steel rebars are plain carbon steels, no alloying elements were added. The Cu, Cr, and other foreign elements remained in these steels below the limit for alloying effects. But there is a difference between the grain size and shape of two steel rebars. From the hall-petch relation, it can be said that, the smaller the grains of steels, the stronger the steels [45, 61]. So, small ferrites and pearlites of steel 2 may increase the strength of it than steel 1. The greater percentage of pearlite can also improve the strength of steels [62]. As from the Fig. 4.6b, it has been seen that steel 2 contained larger amount of pearlite than steel 1, so steel 2 may have greater strength than steel 1. If the strength increases, the ductility or percentage of elongation decreases, so, steel 2 may has smaller ductility than steel 2.

But, if steel 1 and 2 have similar percentage of carbon, then how could the percentage of pearlite be different. If the cooling rate from the upper critical temperature or austenite zone is high, then the amount of pearlite can increase [63]. During the quenching it may possible to have different cooling rate for different steels for the variations in water flow. So, steel 2 may show higher strength than steel 1.

If the temperature of the rolled bar after last pass is higher, that is, if the temperature of the austenite zone is higher before entering the quenching box, the austenite grains are large, and this large austenite grain gives rise to large ferrite and pearlite grains after transformation. So, for steel 1 it may be possible that before transformation the austenite grains were larger and resultantly it transformed into large grains of ferrite and pearlite. So, steel 1 has lower strength than steel 2.

On the other hand, in Fig. 4.7b, it is seen that, steel 3 contains smallest grains of ferrite and pearlite. The percentage of pearlite is also greater than steel 2. The shape of ferrite grains are not equiaxed. Steel 4 in Fig. 4.8b, showed somehow a different structure of the core than the rest three steel rebars.

There are a lot of big grains of different structure. The percentage amount of ferrite is lower than steel 3, 2 and 1. The shape of ferrite grains are not equiaxed. The grain sizes of steel 3 and 4 are small with some amount of large grains. The amount of pearlite is greater than others. The different structure may be the Widmanstätten structure. From the table of composition it is shown that, steel 3 and 4 have similar carbon contents but greater than steel1 and 2. So, higher carbon contents gave relatively higher strength to steel 3 and 4 than steel 1 and 2. Additionally, the small grains also contribute the higher strength of steel 3 and 4. In steel 4 some Widmanstätten structures were found. The Widmanstätten structure consists of fine ferrite and pearlite like quasieutectoid [64, 65]. Theoretically, the Widmanstätten structure is undesirable for steels. It has been said that this structure has negative influence on impact properties. Though, this structure increases strength of metals but develops brittleness in steels. However, in some cases it has been found that, steels with Widmanstätten structure have satisfactory properties [64, 65]. The highest strength for steel 4 is possibly due to this structure also. It is said, a microstructure of steel resulting Thomson structures or Widmanstätten structures when it cools at a critical cooling rate from extremely high temperature [65].

Fine austenite grains give rise to fine martensites. The steels containing fine martensite have high hardness and strength. From Fig. 4.5a and 4.6a it is seen that steel 2 has finer martensite than steel 1. The black portions of the microstructures indicate fine low carbon martensite. However, from the light optical microscopy (LOM) it is not well possible to measure the fineness of martensite lath but qualitatively it can be understood. Steel 2, 3 and 4 contained finer low carbon martensite than steel 1. As it has shown for core that the grain size of ferrite of steel 1 is larger than the rest of the steels, so for case the martensites of steel 1 are less fine than others, because coarse austenite grains produce coarse ferrites and martensites. If the percentage amount of ferrite colony increases in cases of steel rebars, the strength of the case area tend to decrease. Fine martensites give higher strength to the case. Again, the percentage of carbon of steel also gives effect to the strength of martensites. With increasing the percentage of carbon in steel the strength of martensites increases. The polygonal white area is ferrite colony, as the steel rebars are very low carbon steels which contain 0.18% of carbon in average. The Isothermal transformation (I-T) diagram moves leftwards and the critical cooling rate (CCR) increases for low carbon steel. In this case, during quenching, practically some ferrites are formed. From the Figs. 4.5a, 4.6a, 4.7a, and 4.8a, it is assumed that, the amount percentage of ferrite colony is 5-8%. If the percentage of ferrites (soft phase) increases, the strength and hardness of the case decreases. But, the 5% ferrites affect a little to lower the strength and

hardness of steels. Now, in figure 4.5a, the martensitic lathe is coarser than others and the percentage of carbon is lower than steel 3 and 4, so the strength and hardness will be lesser than steels 2, 3 and 4. Though steel 2 and 1 has similar percentage of carbon, but the grain size of steel 2 is finer than steel 1. So, steel 2 has higher hardness and strength than the former. The percentage of carbon of steels 3 and 4 is higher than steels 1 and 2. So, higher carbon gives high strength to martensites. Additionally, the martensites are finer than steels 1 and 2. So, steel 3 and 4 have higher hardness and strength according to its microstructures and percentage of carbon. The quenching temperature determines the martensitic grain size and hence, lower quenching temperature gives finer austenite grains which transformed to fine martensites and vice versa. In that case, steel 1 may be quenched at higher temperature than others. This resulted to coarser martensite than others which gave it lower hardness and strength than other steels.

4.3 Tensile Properties:

Tensile strength of four types of steel samples has been performed in the Universal Testing Machine. For each type of steels, three specimens have been tested. 20 mm of diameter steel rebar of and 12 inch in length was used as tensile test sample. The gauge length was taken 200 mm. The data produced by the machine is presented in tables below.

4.3.1 Tensile properties of steel rebar keeping the rib as-received:

Three kinds of surface condition for the tensile test of the steel rebars have been experimented. Firstly, the as-received rebars with ribs on surface are directly tested. The test result has been shown in the Table 4.3.

From the table 4.3, it can be seen that the maximum strength has been achieved from the steel 4 with the lowest percentage of elongation which is 11%. All these steels are said to have 500 MPa yield strength from the company. But, experimentally, these steels showed yield stress above 500 MPa. Steels 1 and 3 showed higher ductility than steel 2 and 4. Although, steel 3 has higher ductility, it shows greater strength than steels 1 and 2. Steel 2 has greater strength than steel 1 but lower ductility than both steel 1 and 3.

Table 4.3: Tensile properties of various grouped reinforcing bars with rib.

Steel ID	Yield Stress (MPa)	Tensile Stress (MPa)	Elongation (%)
1	543	639	14.5
2	556	659	12
3	554	675	14
4	594	723	11

4.3.2 Tensile properties of steel rebars without rib:

The ribs of some specimens of steel bars have been peeled off from the surface by machining keeping the case and core intact. Though, some portions of the case of the samples have been removed as a result of machining. The machined samples are 18 mm in diameter and 12 inch long. These samples were tested in UTM again. The gauge length was taken 200 mm of the length. The tensile test results of steel rebars without ribs has been shown in Table 4.4.

Table 4.4: Tensile properties of various grouped reinforcing bars without rib.

Steel ID	Yield Stress (MPa)	Tensile Stress (MPa)	Elongation (%)
1	530	658	16
2	519	636	15
3	545	669	17
4	530	666	12

Table 4.4 states that, the maximum strength has been achieved from the steel 3 with the highest percentage of elongation which is 17%. The second highest strength is achieved by steel 4 but the lowest amount of ductility with 12% of elongation. Tensile strength of steel 1 is slightly lower than that of steel 4 but yield stress is equal. Steel 1 shows greater percentage of elongation than steels 2 and 4 in this surface condition. Steel 2 shows the lowest strength than steels 1, 3, and 4, but the

percentage of elongation is greater than steel 4. This table also states that the ribs on surface have effect on decreasing ductility of the rebars. However, due to removing ribs and for loss of some mass of those rebars strength has been reduced to some extent. The rib has small surface area; it cools faster and contains fine martensites. Fine martensites are very strong. To remove away the ribs, the fine martensites are lost. Thus, the strength of the steel bars without ribs decreases.

4.3.3 Tensile properties of steel rebars without hardened zone (Case):

Tensile strength of steel rebars with the core of same chemical composition has been determined. In that case, the ribs and hardened zone and some portion of the transition zone of rebars are removed by machining. Table 4.5 presents the tensile test results without hardened zone. The specimens of steels are 15 mm in diameter and 12 inch long with 200 mm gauge length.

Table 4.5 reveals that, the maximum strength has been achieved from the steel 4 with the lowest ductility of 15 percentage of elongation. The yield strengths of steel 1 and 3 are same. The ductility increases of steels 4, 3, 2, and 1 in ascending manner. The ferrite and pearlite structure may cause the improvement of ductility of steels 1 and 2. The tensile strength of steel 3 is greater than steels 1 and 2. Due to refined structure of the core of steel 3 may reduce the ductility than that of other steels.
It is obvious that from the Tables 4.3, 4.4, and 4.5 the highest ductility can be achieved from the softer zone (Core) of the TMT high strength steel rebars. The greater percent of pearlite of steel 2 increases the strength than steel 1. The higher TS of steel 3 and 4 of the softer zone may be due to the refined ferrite, pearlite grains and presence of hard structures in the cores.

Table 4.5: Tensile properties of various grouped reinforcing bars without case.

Steel ID	Yield Stress (MPa)	Tensile Stress (MPa)	Elongation (%)
1	442	552	20
2	448	591	18
3	442	604	17
4	500	663	15

4.4 Rockwell Hardness test:

Rockwell hardness Test is performed for four types of TMT steel rebars. The Rockwell hardness test for hardened zone and softer zone has been performed separately. For hard Case Rockwell C scale is used and for soft core Rockwell B scale is used to measure hardness. Table 4.6 shows the average Rockwell hardness values for both hardened (Case) and softer zones (Core) with the depth of the hardened zone and Carbon Equivalent (CE).

Table 4.6: Rockwell hardness of case and core with carbon equivalent and case depth.

Steel ID	Case Depth, mm	Case Hardness, HRC	Core Hardness, HRB	CE
1	1.80	30.3	86.3	0.33
2	2.00	29.8	86.7	0.35
3	2.10	32.3	90.8	0.36
4	1.95	32.3	91.5	0.34

From the table 4.6, it is said that, higher carbon equivalent gives higher hardness for the steel rebars. Steel 3 has the highest carbon equivalent having higher case hardness of 32.3 HRC and core hardness of 90.8 HRB. The case hardness of steel 4 is similar to steel 3. Though, steel 4 has slightly lower CE value than steel 3, but it shows slightly greater core hardness of 91.5 HRB than steel 3. Steel 2 has lower case hardness and lower core hardness than steels 3, and 4, although it has higher CE than steel 4. Again, Steel 1 has lower CE than steel 2 but, in spite of this, steel 1 exerts greater hardness in case

than steel 2. But, the core hardness of steel 1 is lower than steels 2, 3, and 4. So, a little anomaly is witnessed in Rockwell hardness results for the steel rebars.

4.4.1 Graphical representation of hardness values of steels:

The Rockwell hardness values for all steels are plotted for both softer zone and hardened zone respectively. These plots corresponding to core hardness and case hardness are presented in Figs. 4.9 to 4.16.

4.4.1.1: Core Hardness:

For softer zone (Core) of the steels, the measured hardness in Rockwell B scale has been plotted against the distance along the diameter of the core area after the case boundary. In that case, the transition zone (TZ) was included with core. Hence, the variation of hardness value across the TZ has been described in the graphs for all types of steel bars.

Figs. 4.9 to 4.12 show the hardness values of the softer zone of steels 1 to 4 respectively. The two ends of the core show higher hardness values which belongs to the transition zone (TZ) of the rebars. This observation is true for both steels. The reason is that, TZ areas closer to the case was cooled at a higher rate, which caused finer and strong microstructures and more residual stress in that areas. The hardness of the middle portion of the core diameter remained more or less constant. All types of steel bars showed similar pattern.

4.4.1.2: Case Hardness:

From the Fig. 4.13 to Fig. 4.16, the hardness of the hardened zone has been graphically presented. Rockwell hardness values in C scale was plotted against the linear peripheral distance of the hardened zone. The periphery of the circular steel bars that is $2\pi r$ (where r is the radius of the steel bar, and π (pi) is the constant) was calculated and considered as the linear distance of the abscissa.

All figures corresponding to the hardness of the case showed more or less constant values with a little deviation. The case structure may contain (some retained austenite and low carbon bainite) / ferrite colony with the hardest tempered low carbon martensite phase, so a little variation of hardness value appeared in the test result among the steel rebars. This variation in hardness and in microstructures was possibly resulted from the non-uniform cooling rate during quenching. During the heat treatment operation, finally hot rolled steel bars were quenched in a water chamber, where water is sprayed from all sides under high pressure. The quenching action depends on the rate of cooling. In the case

of mass scale industrial production, it is not easy to confirm uniform cooling rate for all surface areas. The trendlines from the Figs. 4.13 and 4.16 indicate that, steel 1 and steel 2 have similar but lower case hardness of HRC 30 compared to steel 3 and steel 4 which have higher case hardness of HRC 32.

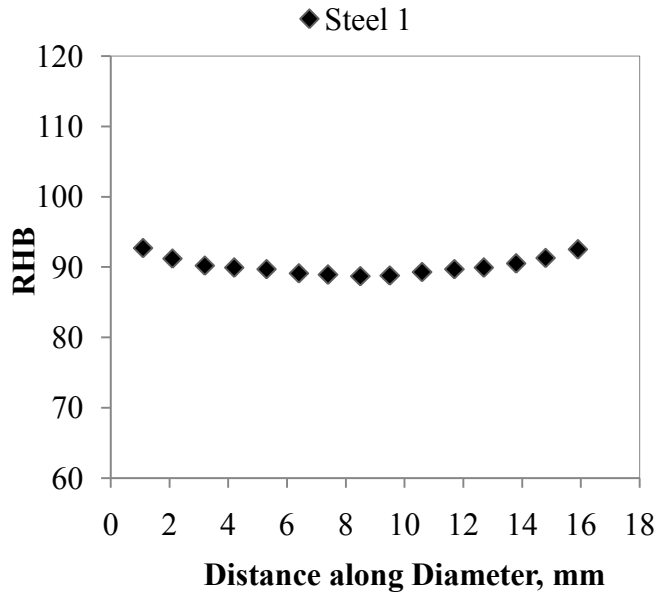

Figure 4.9: Rockwell hardness (HB) of core along the diameter of core of steel 1.

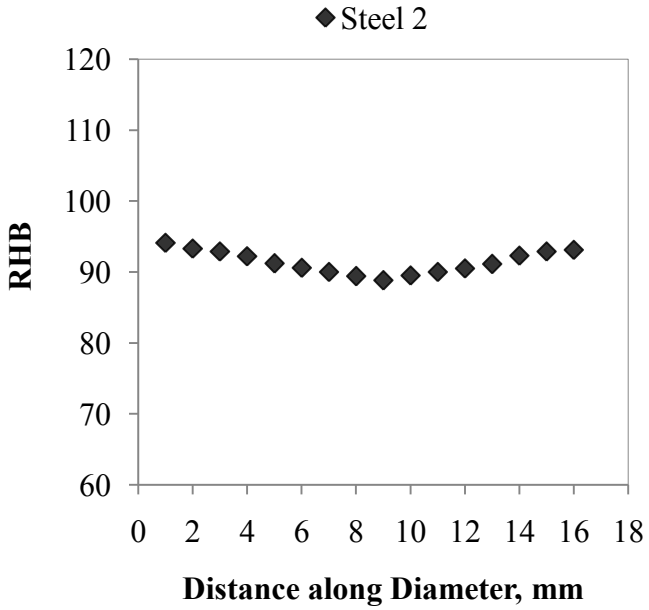

Figure 4.10: Rockwell hardness (HB) of core along the diameter of core of steel 2.

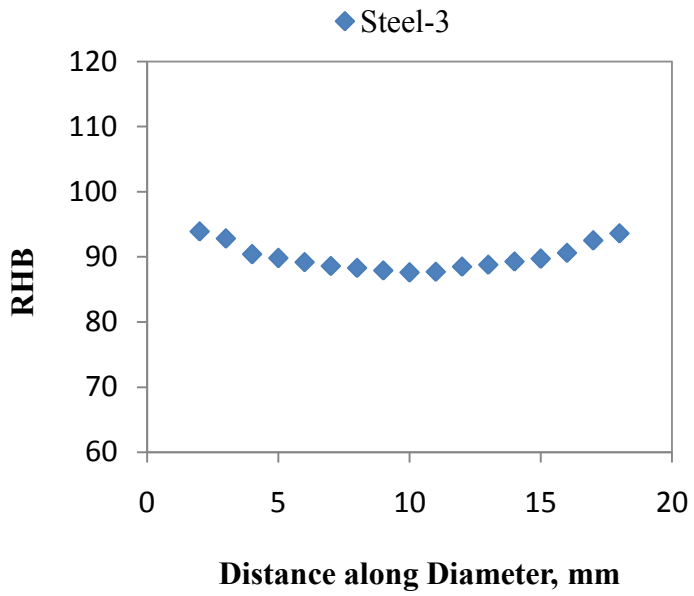

Figure 4.11: Rockwell hardness (HB) of core along the diameter of core of steel 3.

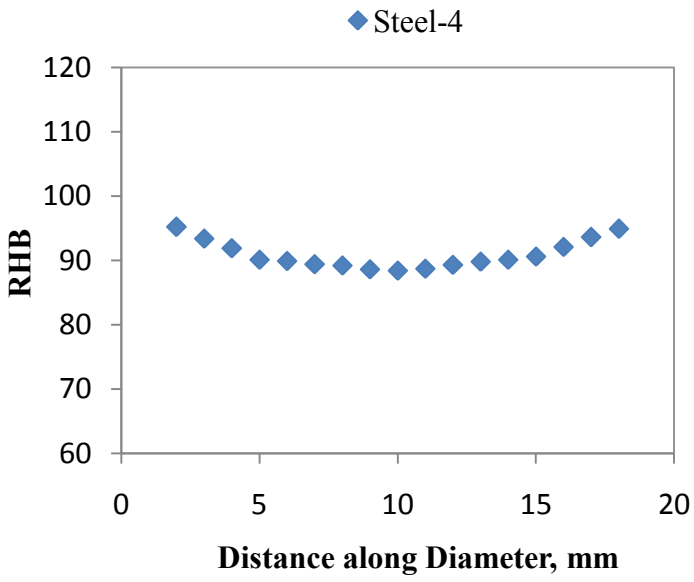

Figure 4.12: Rockwell hardness (HB) of core along the diameter of core of steel 4.

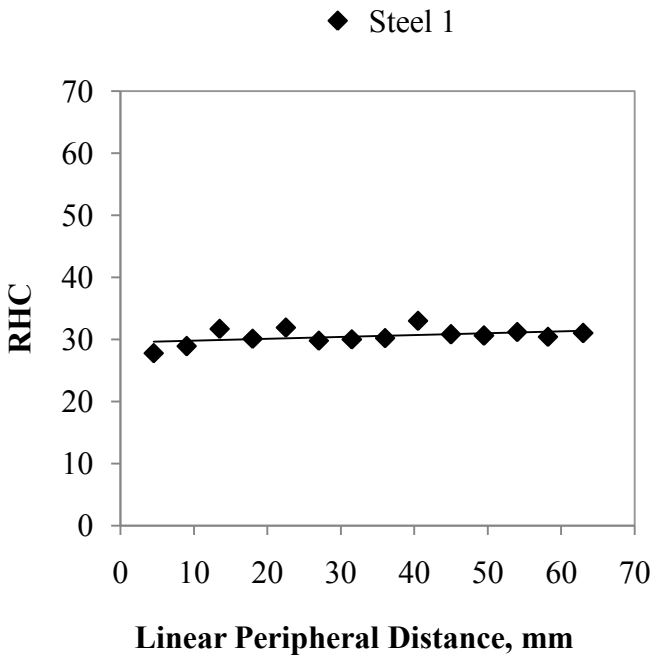

Figure 4.13: Rockwell hardness (HC) of case along the periphery of steel 1.

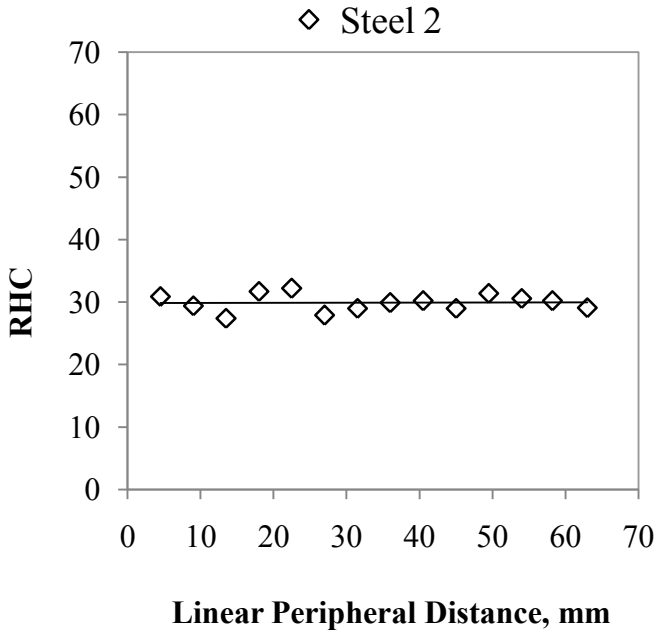

Figure 4.14: Rockwell hardness (HC) of case along the periphery of steel 2.

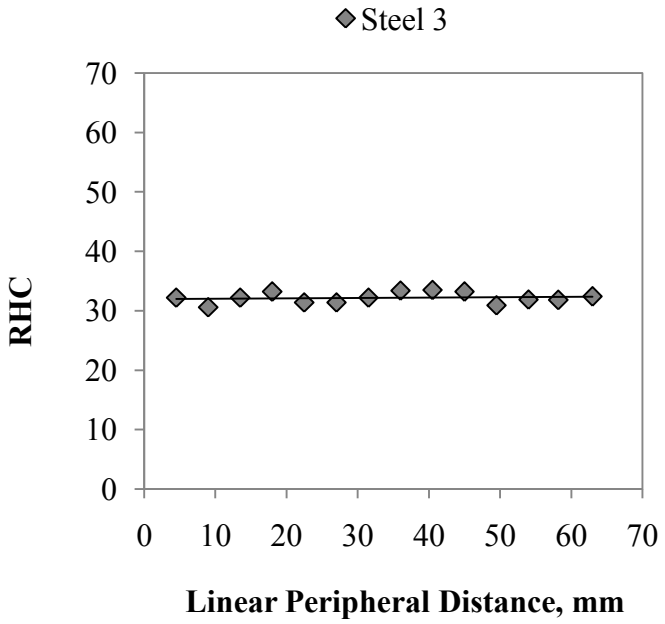

Figure 4.15: Rockwell hardness (HC) of case along the periphery of steel 3.

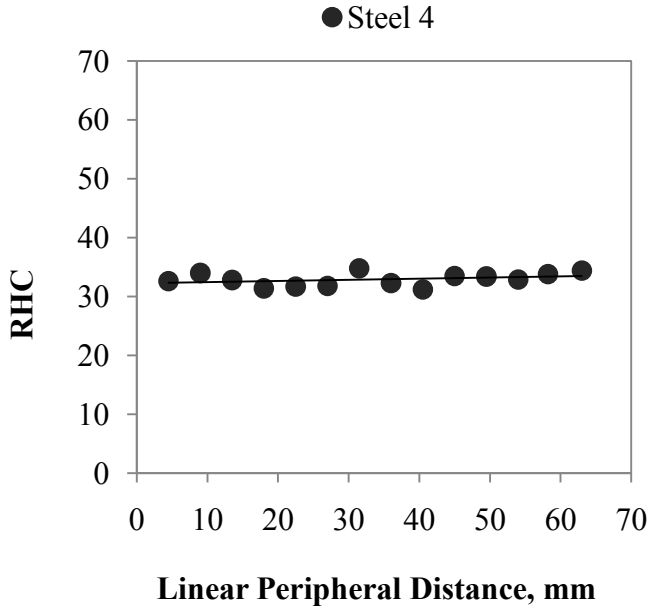

Figure 4.16: Rockwell hardness (HC) of case along the periphery of steel 4.

4.5: Correlation of Tensile properties with Hardness:

4.5.1: Conversion of Rockwell hardness values into tensile strength:

The Rockwell hardness is converted into tensile strength of steel bars according to the hardness conversion chart followed the standard of ASTM [54, 55]. This is an approximate tensile strength of steels converted from the Rockwell hardness. The converted tensile strength values are then plotted against the corresponding Rockwell hardness values of the samples. Linear trendlines and linear regression equations for each graphical plot of the samples is determined. These steps are followed for both case and core separately.

Core:

The Rockwell hardness values of the core of steels have been put down in the abscissa and the corresponding tensile strength values converted from this hardness of the core have been put onto the ordinate. The scattered graph generated from those values of Rockwell hardness and respective tensile strength gave an equation correlating the hardness as x, with the approximated tensile strength of core as y. The R-squared value represents how best those data fitted in the linear regression trendline. This R-squared is stated by the goodness-of-fit or, coefficient of determination. The higher the R^2 value, the better those data fit with the model.

This equation follows the linear regression equation $y= mx + c$. here, y refers the estimated tensile strength, x refers the Rockwell hardness of core, m and c are constant. Constant c is related to different kind of lattice friction during deformation of materials. This term depends on lattice structure, microstructures, chemical composition, load types, pressure, etc. The coefficient of x in these equations varies. This represents the ratio of tensile strength to Rockwell hardness of the material. This ratio for hardened zone of these steels indicates which steel have a good strength with better ductility or a good strength without ductility.

From the Figs. 4.17-4.20, it can be stated that, the coefficient m is lower for the core than the case. All four types of steel have near values of m for core. But these m values showed an ascending manner from steel 1 to steel 4. Steel 1 has the lowest m value and steel 4 reveals highest value of m. The constant c showed highest but negative value for the core than the case. Steel 1 and 2 has lower c value than steel 3 and 4.

Case:

The Rockwell hardness values of the case of steels have been put down in the abscissa axis and the corresponding tensile strength values converted from this hardness of the case have been put onto the ordinate. The scattered graph generated from those values of Rockwell hardness and respective tensile strength gave an equation correlating the hardness as x, with the approximated tensile strength of hardened zone as y, of TMT high strength steel bars. The R-squared value represents how best those data fitted in the linear regression trendline. This R-squared is stated by the goodness-of-fit. The higher the R^2 value means the better those data fit with the model.

This equation follows the linear regression equation y= mx + c. here, y refers the estimated tensile strength, x refers the Rockwell hardness of case, m and c are constant. Constant c is related to different kind of lattice friction during deformation of materials. This term depends on lattice structure, microstructures, chemical composition, load types, pressure, etc. The coefficient of x in these equations varies. This represents the ratio of tensile strength to Rockwell hardness of the material. This ratio for hardened zone of these steels indicates which steel have a good strength with better ductility or a good strength without ductility.

In Figs. 4.21-4.24, it is seen that, steel 1 and 2 shows lower coefficient, m, than steel 3 and 4. The c constants are higher for steel 1 and 2 than steel 4. Steel 3 shows negative value of c.

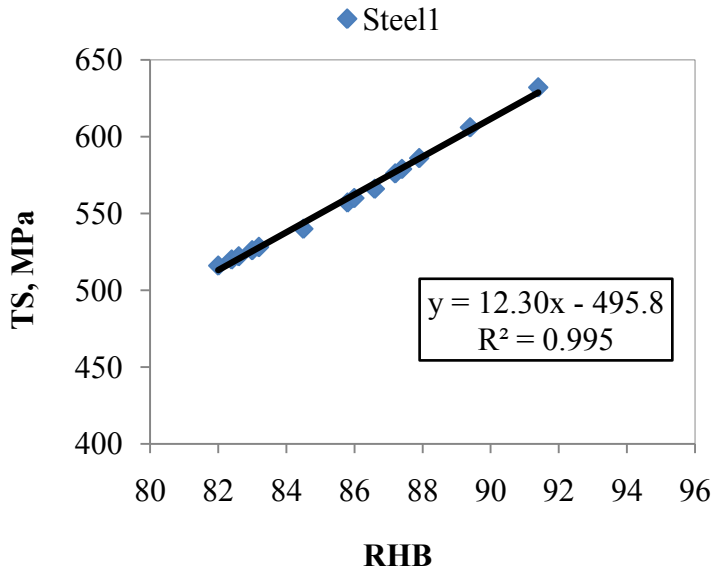

Figure 4.17: Hardness of core vs. corresponding converted tensile strength of steel 1.

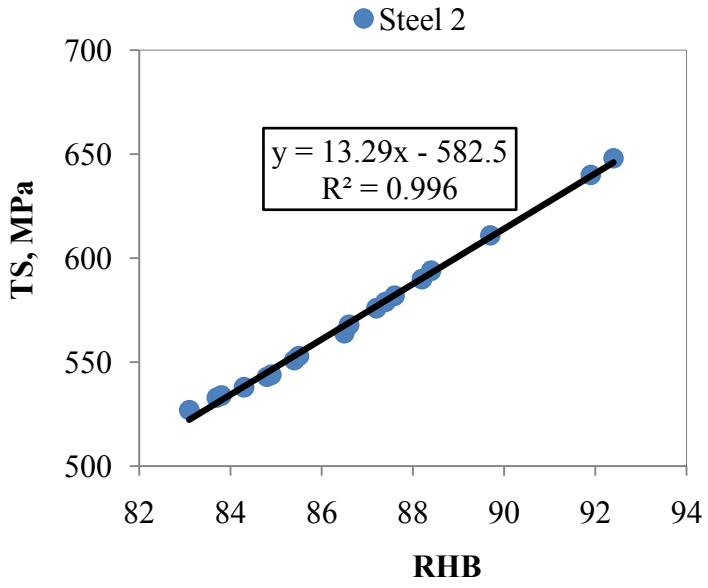

Figure 4.18: Hardness of core vs. corresponding converted tensile strength of steel 2.

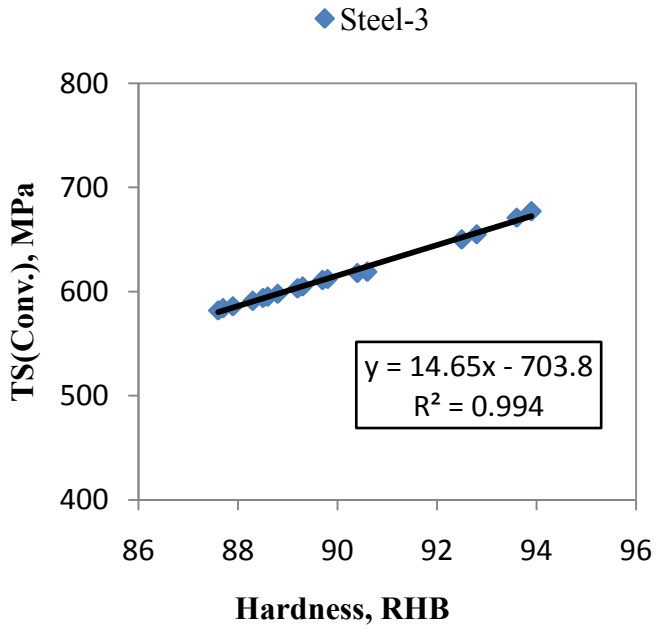

Figure 4.19: Hardness of core vs. corresponding converted tensile strength of steel 3.

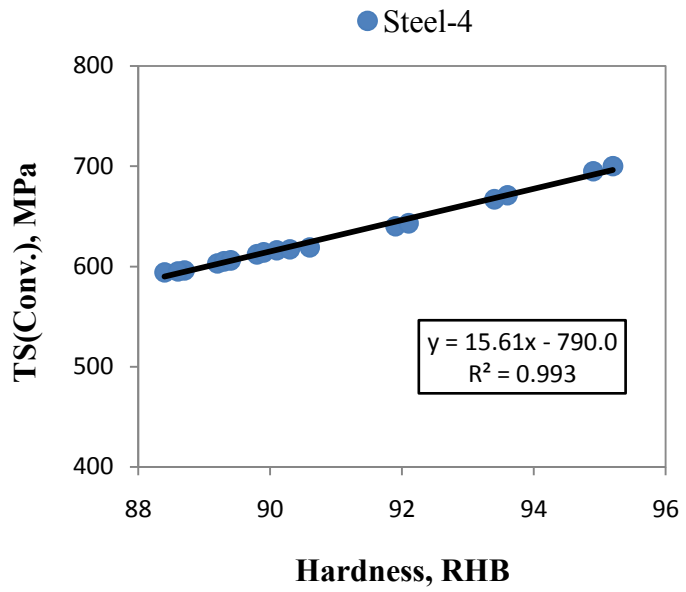

Figure 4.20: Hardness of core vs. corresponding converted tensile strength of steel 4.

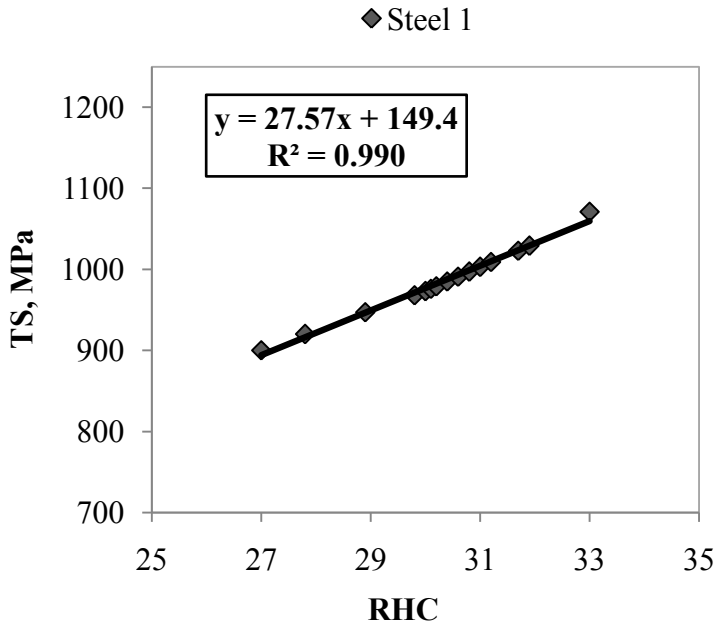

Figure 4.21: Hardness of case vs. corresponding converted tensile strength of steel 1.

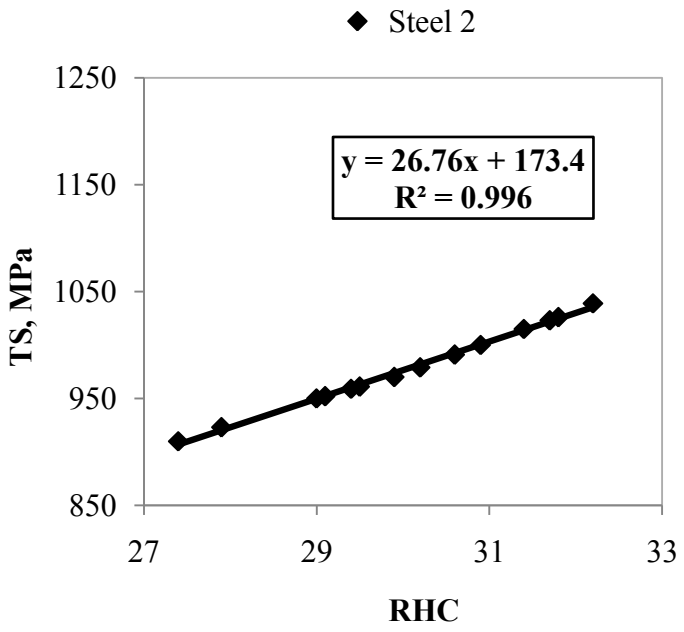

Figure 4.22: Hardness of case vs. corresponding converted tensile strength of steel 2.

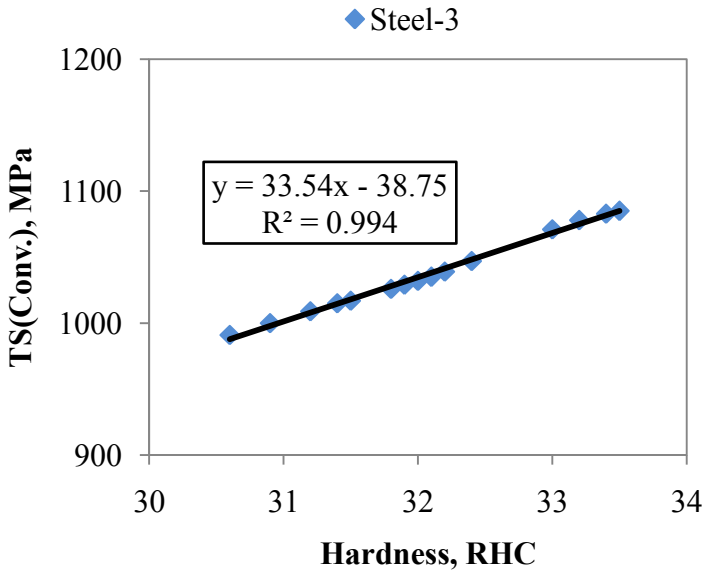

Figure 4.23: Hardness of case vs. corresponding converted tensile strength of steel 3.

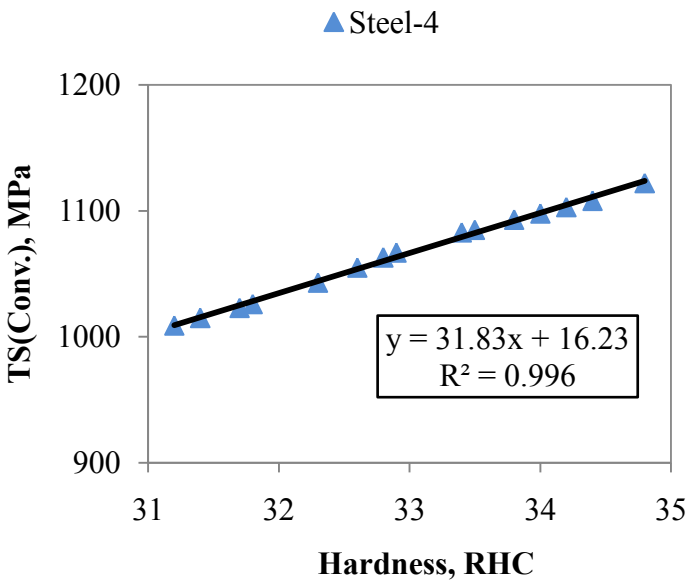

Figure 4.24: Hardness of case vs. corresponding converted tensile strength of steel 4.

Calculating the total tensile strength of the steel bars:

After generating those equations of Rockwell hardness and tensile strength of the case and core areas separately the total tensile strength has been calculated for each type of steel rebars. The equations of case and core were infused by simple law of mix theory to determine the approximated and predicted tensile strength for whole steel bar. This calculated tensile strength nearly followed the order for the steel bars like the order of tensile strength resulted from tensile tests. Here, steel 3 showed the highest strength and steel 1 showed the lowest. Steel 4 had higher strength than steel 2. The calculated tensile strengths of the steel rebars are higher than their experimented values. The maximum deviation of tensile strength value from experimented value shown by steel 3 was 16.3 percent. Steel 2 and 4 deviated lower than steel 3 which are 8.4 and 8 percent respectively. Steel 1 shows 10 % deviation.

TS (MPa) of steel 1 = [12.302 x average hardness of core in RHB - 495.85] x proportion of core + [27.572 x average hardness of case in RHC + 149.49] x proportion of case

= [12.302 x 86.3 - 495.85] x 0.67 + [27.572 x 30.3 + 149.49] x 0.33

= 379 + 325

= 704 MPa (10% higher compared to tensile test result)

TS (MPa) of steel 2 = [13.296 x average hardness of core in RHB - 582.55] x proportion of core + [26.796 x hardness of case in RHC + 173.43] x proportion of case

= [13.296 x 86.7-582.55] x 0.64 + [26.769 x 29.8 + 173.43] x 0.36

= 364.9 + 349.6

= 714.5 MPa (8.4% higher compared to tensile test result)

TS (MPa) of steel 3 = [14.65x average hardness of core in RHB - 703.8] x proportion of core + [33.54x hardness of case in RHC - 38.75] x proportion of case

= [14.65 x 90.8 -703.8] x 0.62 + [33.54 x 32.3 – 38.75] x 0.38

= 388.4 + 396.9

= 785.3 MPa (16.3 % higher compared to tensile test result)

TS (MPa) of steel 4 = [15.61x average hardness of core in RHB- 790.0] x proportion of core + [31.83x hardness of case in RHC + 16.23] x proportion of case

= [15.61 x 91.5 -790.0] x 0.65 + [31.83 x 32.3 + 16.23] x 0.35

= 414.9 + 365.5

= 780.4 MPa (8% higher compared to tensile test result)

The reason behind this is that the mathematical models of the steel bars were developed considering their hardness values and the corresponding tensile strength values of smooth samples. However, in the present research, steel bars were used with ribs and also that hot rolled steel surface is relatively rough, Fig.4.25.

Figure 4.25: Hot rolled steel bars with ribs and oxidized surfaces.

Both the ribs and oxidized rough surface act as stress concentrators. As a result, tensile strength results obtained from conventional tensile tests are relatively lower than that obtained by the developed mathematical models. However, for both steels, this deviation from the tensile test results

is consistent. Some other researchers also developed mathematical models for tensile strength of steels in terms of their hardness values and they also mentioned this type deviation [14, 56].

The linear correlation of Rockwell hardness to tensile strength converted from hardness has been presented from Figs. 4.17 to 4.24 for both case and core respectively. From these figures, the linear regression coefficients, regression constants of those equations of the steels for case and core have been tabulated below.

Table 4.7: The equation parameters of the mathematical correlation models of TS and hardness.

Position	Steel ID	Regression coefficient	Regression Constant	Equations
Core	1	12.30	- 495.8	y = 12.30x - 495.8
	2	13.29	- 582.5	y = 13.29x - 582.5
	3	14.65	- 703.8	y = 14.65x - 703.8
	4	15.61	- 790.0	y = 15.61x - 790.0
Case	1	27.57	+ 149.4	y = 27.57x + 149.4
	2	26.76	+ 173.4	y = 26.76x + 173.4
	3	33.54	- 38.75	y = 33.54x - 38.75
	4	31.83	+ 16.23	y = 31.83x + 16.23

From Table 4.7 it has been seen that, for core, the regression coefficient of steel gradually increases from steel 1 to steel 4, although, the difference between all coefficients of the steel bars is very low. That means, for a given number of hardness, tensile strength for the core will increase from steel 1 to steel 4 gradually. From the tensile test results of the steel bars with core tabulated in Table 4.5, it is seen that this manner of increasing TS for cores completely follow the tensile test results of the steels. On the other hand, for case, the coefficients of steel 1 is greater than steel 2 and that of steel 3 is greater than steel 4. The maximum coefficient is of steel 3 for case and the minimum coefficient is of steel 2. By recalling the tensile test data of the steels with case and core from Table 4.4, it is seen that, for case the TS is maximum for steel 3 and minimum for steel 2. In this case, the manner of the coefficients increase and decrease also follow the tensile test results. But, when the tensile tests were

done with ribs of the steels, the strength increased ascending from steel 1 to steel 4 which presented in Table 4.3. So, the combined effects of case and core and the size and distribution of ribs for the thermo mechanically treated steels has slightly modified the strength ultimately. The tensile tests results show good agreement with microstructures of case and core of the steels and the converted TS from hardness have been follow the manner of the tested TS results. So, the linear regression model of converted TS and hardness has shown strong dependency with the microstructures of the steels.

4.5.2: Conversion of hardness values into Yield strength:

Unlike the tensile strength, the yield strength cannot be converted from the standard conversion chart. In this study, we followed two methods to determine yield strength from the experimental hardness values of the steels. All the calculations have been done for both Case and Core of the steels separately.

4.5.2.1 Correlation of Rockwell Hardness with yield strength from the ratio of TS to YS:

In first method, the ratio of tensile strength to yield strength determined from the mechanical tests has been utilized. For case the tensile to yield strength ratio obtained from the tensile tests result of the steels without rib (leaving the case and core) has been used. And for Core that TS/YS ratio which was obtained from the tests result of those steels without case (keeping core behind) has been used. Now, the converted tensile strength has been converted to yield strength using the ratio. The converted tensile strength obtained from the Rockwell hardness of the steels following the standard chart of conversion. This converted yield strength with its corresponding values of Rockwell hardness has been plotted. From this plot a linear regression equation has been determined correlating the Rockwell hardness and yield strength. This procedure has been executed for all four types of steel and for their case and core separately. Thus, total 8 equations (tabulated in Table 4.8) have been developed from the plots. After that, the total yield strength for the steels combining case and core of each steel rebar has been calculated adding the weighted means of the yield strengths of case and core. The plot of the Rockwell hardness versus converted yield strength has been presented in Figs. 4.26 to 4.33 below. The calculations of determining the total yield strength with its percent of deviation from the tests values have also been presented as follows.

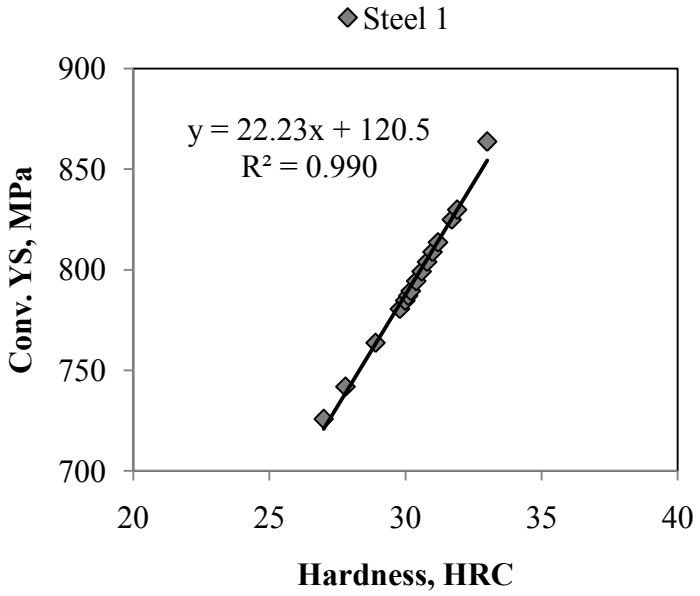

Figure 4.26: Hardness of case vs. corresponding converted yield strength of steel 1.

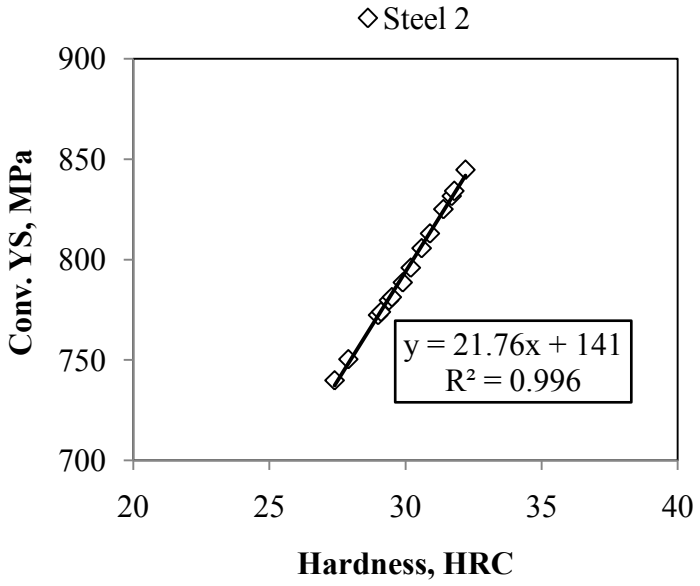

Figure 4.27: Hardness of case vs. corresponding converted yield strength of steel 2.

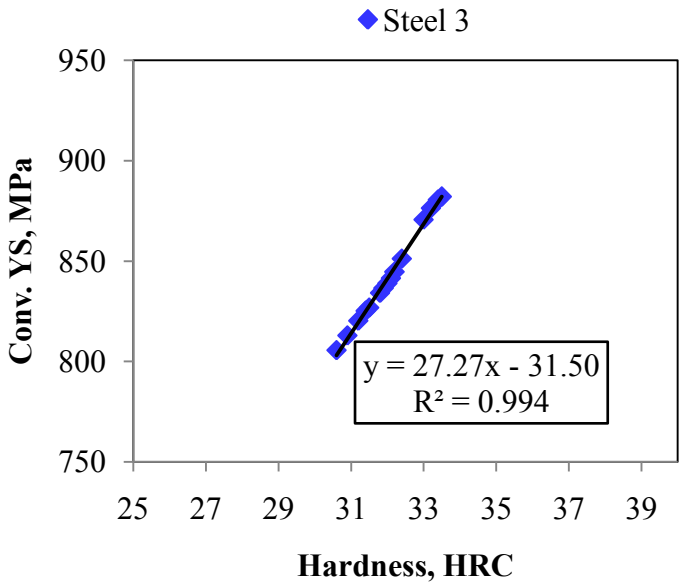

Figure 4.28: Hardness of case vs. corresponding converted yield strength of steel 3.

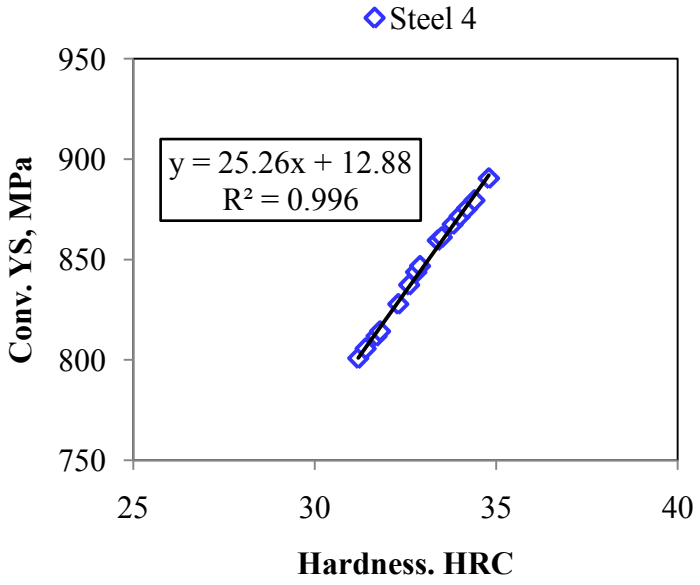

Figure 4.29: Hardness of case vs. corresponding converted yield strength of steel 4.

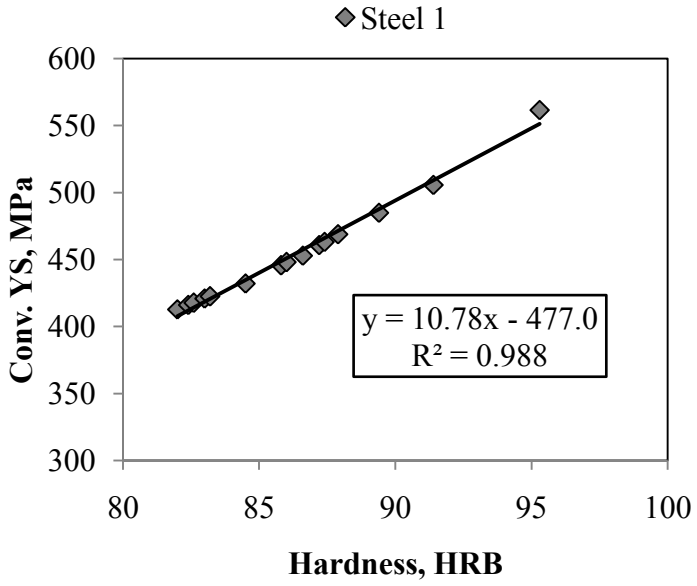

Figure 4.30: Hardness of Core vs. corresponding converted yield strength of steel 1.

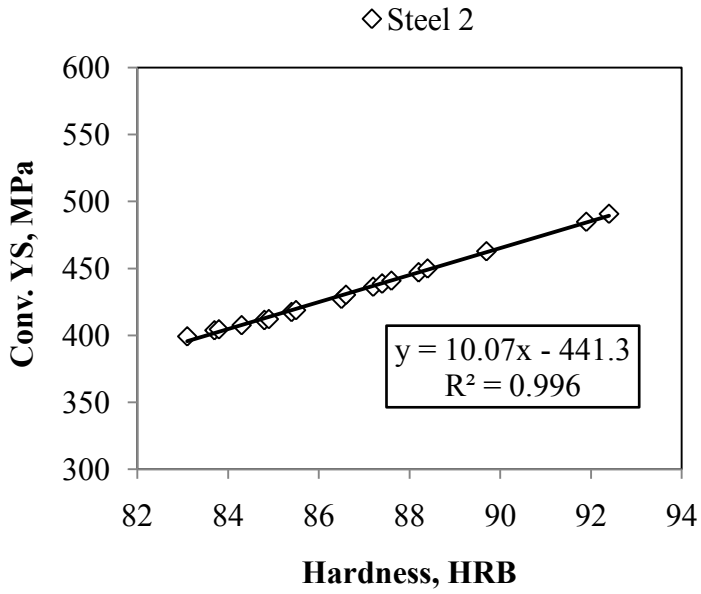

Figure 4.31: Hardness of Core vs. corresponding converted yield strength of steel 2.

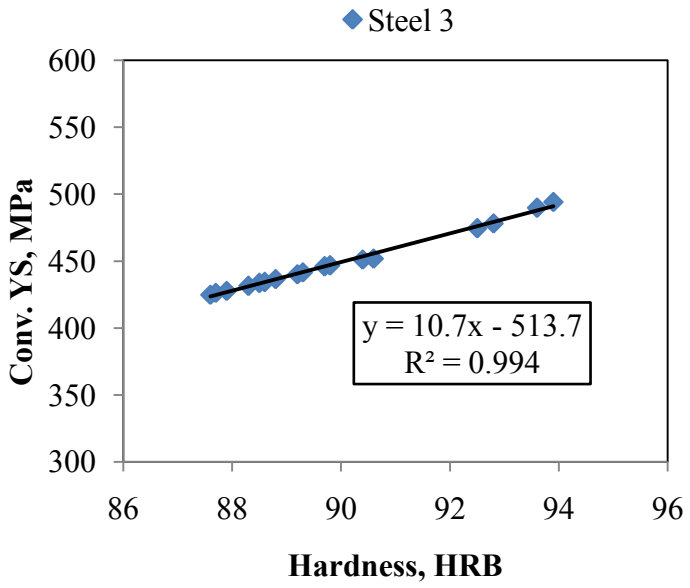

Figure 4.32: Hardness of Core vs. corresponding converted yield strength of steel 3.

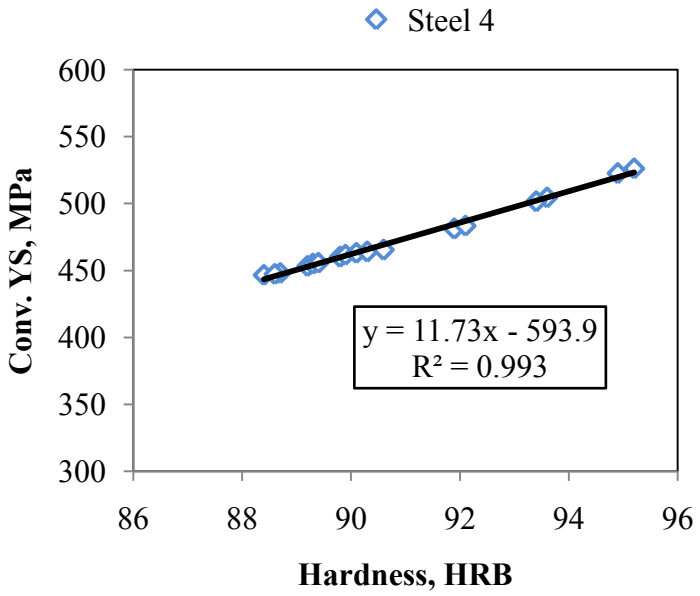

Figure 4.33: Hardness of Core vs. corresponding converted yield strength of steel 4.

Calculating the total Yield Strength of the steel bars:

After generating those equations of hardness and yield strength of the case and core areas separately the total yield strength has been calculated for each type of steel. The equations of case and core were infused by simple law of mix theory to determine the approximated and predicted yield strength for whole steel bar. The order of the calculated yield strengths for steel rebars nearly followed the order of yield strengths resulted from tensile test. That is, steel 3 shows the highest yield strength, and steel 1 shows the lowest yield strength. Steel 4 has higher yield strength than steel 2. These calculated yield strength values of the steel rebars are higher than their tested values. The maximum deviation of yield strength value from experimented value shown by steel 3 is 9 %. Steel 2 and 4 deviated lesser than steel 3 which are 0.8 and 1.2 percents respectively. Steel 1 shows 4 % deviation. But these deviations are lower than the deviation in case of calculated tensile values of the steel rebars from hardness.

YS (MPa) of steel 1 = [10.78 x average hardness of core in RHB - 477] x proportion of core + [22.23 x average hardness of case in RHC + 120.5] x proportion of case

= [10.78 * 86.3 - 477] * 0.67 + [22.23 * 30.3 + 120.5] * 0.33

= 565.76MPa (4% higher compared to tensile test result)

YS (MPa) of steel 2 = [10.07 x average hardness of core in RHB - 441.3] x proportion of core + [21.76 x hardness of case in RHC + 141] x proportion of case

= [10.07 * 86.7 - 441.3] * 0.64 + [21.76 * 29.8 + 141] * 0.36

= 560.53MPa (0.8% higher compared to tensile test result)

YS (MPa) of steel 3 = [10.7 x average hardness of core in RHB - 513.7] x proportion of core + [27.27 x hardness of case in RHC - 31.50] x proportion of case

= [10.7 * 90.8 - 513.7] * 0.62 + [27.27 * 32.3 -31.50] * 0.38

= 606.62MPa (9 % higher compared to tensile test result)

YS (MPa) of steel 4 = [11.73x average hardness of core in RHB- 593.9] x proportion of core + [25.26 x hardness of case in RHC + 12.88] x proportion of case

= [11.73* 91.5 - 593.9] * 0.65 + [25.26 * 32.3 +12.88] * 0.35

= 601.68MPa (1.2% higher compared to tensile test result)

Table 4.8 presents the regression coefficients, regression constants and the linear equations obtained from the mathematical models of the converted yield strength and Rockwell hardness of the steel rebars. The case and core are separately correlated for the TMT steel rebars. From the Table 4.8, it is clear that, for core, the regression coefficients are similar fro steel 1 and steel 3. Steel 4 shows highest coefficient and steel 2 has the lowest coefficients. But, the difference among the all coefficients is very small. That means for a given Rockwell hardness value, steel 4 will show the maximum yield strength and steel 2 will show the minimum yield strength. Steel 1 will show more or less similar with steel 3. Recalling the Table 4.5, it has been seen that, the pattern of converted yield strength for the steel rebars nearly fits with the pattern of YS obtained from tensile test results. Instead that, steel 2 in tensile test showed slightly greater value than steels 1 and 3. On the other hand, for case, the coefficients of steel 1 is greater than steel 2 and that of steel 3 is greater than steel 4. The maximum coefficient is of steel 3 for case and the minimum coefficient is of steel 2. By recalling the tensile test data of the steels with case and core from Table 4.4, it is seen that, for case, the YS is maximum for steel 3 and minimum for steel 2. The similar YS of steels 1 and 4 have been obtained from tensile test results, although the regression coefficients of steel 4 is slightly greater than steel 1. From the view point of microstructures chemical compositions of the steels, it can be said that, the coarse ferrite grain, lower percentage of pearlite, coarser martensitic lath and lower carbon martensite have exerted lower yield and tensile strength of steel 1. For steel 3, increased amount of pearlite, finer grain of ferrite, finer martensite, and higher percentage of carbon increased both yield and tensile strength. The presence of different structures in core of steel 4, higher percentage of carbon, finer grain of ferrite, increased percentage of pearlite and finer martensite developed higher strength than steel 1. But with increasing the hardness and strength of steels 2 and 4, the percentage of elongation has been decreased. For steel 3, percentage of elongation did not decrease in spite of having higher strength and hardness.

Table 4.8: The equation parameters of the mathematical correlation models of YS and hardness.

Position	Steel ID	Regression coefficient	Regression Constant	Equations
Case	1	22.23	+ 120.5	y = 22.23x + 120.5
	2	21.76	+ 141.0	y = 21.76x + 141.0
	3	27.27	- 31.50	y = 27.27x - 31.50
	4	25.26	+ 12.88	y = 25.26x + 12.88
Core	1	10.78	- 477.0	y = 10.78x - 477.0
	2	10.07	- 441.3	y = 10.07x - 441.3
	3	10.70	- 513.7	y = 10.70x - 513.7
	4	11.73	- 593.9	y = 11.73x - 593.9

4.5.2.2 Correlation of Vickers hardness with yield strength using empirical equations:

E. J. Pavlina and C. J. Van Tyne [40] suggested simple linear relationships to estimate the ultimate tensile strength and yield strength using the Vickers hardness number for steels. They correlate the yield strength to Vickers hardness according to the variations of microstructures. They divided the microstructures of steels into three categories: (1) martensitic microstructures, which include as-quenched and quenched and tempered martensite, (2) non-martensitic microstructures, which include ferrite/pearlite, bainite, and acicular ferrite, and (3) complex phase microstructures, which are those that consist of mixtures of ferrite and other phases such as bainite, martensite, or retained austenite. Two regression equations correlating the Vickers hardness to yield strength for the microstructures of martensitic steels and non-martensitic steels were used in this study. Those equations are mentioned below.

$$YS = 110.9 + 2.507\ Hv, \text{ for martensitic structures} \quad (4.2)\ [40]$$

$$YS = -84.8 + 2.646\ Hv, \text{ for non-martensitic structures} \quad (4.3)\ [40]$$

Where, YS refers the yield strength of the steels and H_V indicates the Vickers hardness number.
Table 4.9 presents the calculated values of yield strength from the Vickers hardness no. for the steels used in this study, using the equations mentioned above. The percentage of deviation of calculated values of yield strength from the experimented yield strength values of the steels have been also shown in the table.

Table 4.9: The calculated yield strength from the empirical equations.

Steel ID	%Case area	%Core area	YS (Case), MPa	YS (Core), MPa	Mean YS, MPa	Experimental YS, MPa	% Deviation
1	0.33	0.67	787.99	386.59	519	543	-4.4
2	0.36	0.64	785.23	400.56	539	556	-3
3	0.38	0.62	819.43	444.42	587	554	5.9
4	0.35	0.65	805.43	423.67	557	594	-6.2

From the Table 4.9, it is seen that, for case the yield strength of steels 1 and 2 is lower than that of steels 3 and 4. For core, the YS increases gradually from steels 1 to 3, but, again decreases for steel 4. The YS of the cores follow the order of Carbon equivalent for the steel bars. But, the YS for case, shows a little anomaly. In terms of microstructures of the cores, the YS of the cores show

dependency. But, for case, the YS values show a little incompatibility with microstructures. For the total calculated YS show deviation from that of test data. But, it is true that the calculated YS values show greater agreement with the microstructures. That is, steel 3 has most refined core and case microstructures, which results in higher YS. The steel 4 contains hard structure in core along with mixed fine and coarse ferrites and pearlites, so, resultantly it show greater YS than steels 1 and 2 but lower than steel 3. For steels 1 and 2 the calculated YS show similar agreement with the microstructures. But, the deviations from test values does not sense clearly.

4.6 Observation of Failure modes in Tension through Photography:

The samples of the tensile tests for all steel rebars have been investigated after tensile tests. The fracture surfaces for all surface conditions and all types of steel rebars have been photographed. The pictures of the fracture surface have been presented below.

Figure 4.34: Fracture surface of steel 1 with ribs on surface.

Figure 4.35: Fracture surface of steel 2 with ribs on surface.

Figure 4.36: Fracture surface of steel 3 with ribs on surface.

Figure 4.37: Fracture surface of steel 4 with ribs on surface.

The fracture surface of those steel bars was observed and photographed after tensile tests. The as-received steel bars of four types were examined to study the fracture mode. Figs. 4.34 to 4.37 depict the fracture surface of those steel bars with ribs on surface. Fig. 4.34 belongs to steel 1 and it is seen that steel 1 subjected to both ductile and brittle fracture. The shear failure initiated from the surface of the steel bar of steel 1 and confined to outward from the core. The core of steel 1 underwent a little ductile failure. Similarly steel 2 also faced both kinds of failure, brittle and ductile shown in Fig. 4.35. Near the surface brittle failure initiated in steel 2 which eventually was merged by the ductile fracture in the middle of the core. Steel 3, in Fig. 4.36, showed a large amount of ductile failure with a little brittleness just near the surface. This fracture surface of steel 3 shaped quite like a cup and cone type of ductile fracture mode. The Fig. 4.37 revealed a pure multidimensional shear failure for steel 4 which evident the brittle nature of this steel bar. It looks like a crocodile mouth.

The fracture behaviors without ribs on surface of these steel rebars were also observed and expressed in Figs. 4.38 to 4.41. Fig. 4.38 refers steel 1 without ribs on surface, which showed cup-and-cone type ductile fracture mode. This indicates that ribs reduce ductility of this steel bar. Next Fig. 4.39 reveals the fracture nature of steel 2 without ribs on surface.

Figure 4.38: Fracture surface of steel 1 without ribs on surface.

Figure 4.39: Fracture surface of steel 2 without ribs on surface.

Figure 4.40: Fracture surface of steel 3 without ribs on surface.

Figure 4.41: Fracture surface of steel 4 without ribs on surface.

This Fig. 4.39 shows nearly ductile fracture of this steel with a little brittle nature of failure. Steel 3 also underwent cup-and-cone type ductile fracture which was depicted in Fig. 4.40. Near the case, a

very little amount shear fracture may be occurred. Fig. 4.41 belongs to steel 4 which show a distorted cup-and-cone fracture surface that indicated it subjected to ductile failure with a little brittleness.

From Figs. 4.42 to 4.45, fracture surface of steels without case was presented. All these figures express that the cores of these steels underwent a fully ductile failure when subjected to uniaxial tensile load. But the amount of ductility and the reduction of area near the neck of the cone for all these steels were not similar. Due to the nature of the microstructures, chemical composition and variation in the amount, size, shape and distribution of phases, the variation in percent of elongation may be varied.

Figure 4.42: Fracture surface of steel 1 without Case.

Figure 4.43: Fracture surface of steel 2 without Case.

Figure 4.44: Fracture surface of steel 3 without Case.

Figure 4.45: Fracture surface of steel 4 without Case.

CONCLUSIONS

In this study, from all results and observations the following conclusions are drawn.

1. Variations in case depth, in the area fractions of transition zones (TZ), and cores cause variations in strength and hardness of the TMT steel rebars.
2. The hardness of case area is higher than that of core area for all steel rebars.
3. Having similar percentage of carbon content, some steel bars shows difference in hardness and strength. Steel bars, which show higher hardness, have case containing refined low carbon martensites and core consisting of fine ferrite grains and fine pearlites.

   In some steels, a Widmanstätten structure is observed. This structure gives high hardness and strength of the steels.
4. Having similar level of hardened case depth, higher hardness of case areas induce high tensile strength with reduced ductility. The refined low carbon martensites in case and fine ferrites and pearlites in core increase tensile strength.
5. Excessive high strength ultimately causes poor ductility resulting in unwanted shear type brittle fracture in the reinforcing steel bars.
6. Presence of rib in the TMT steel bars increases yield and tensile strength, decreases percentage of elongation and enhance shear failure in tensile loading.
7. Experimental results revealed that, to minimize the differences in microstructure, tensile properties, fracture behaviours of the TMT steel bars, the heat treatment parameters (quenching temperature, water flow rate, time of quenching, quenching finish temperature, tempering temperature, natural cooling, etc.) should be closely adjusted as per the chemical compositions of the hot rolled bars.
8. Tensile strength values obtained from mathematical models are consistent with that of the tensile strength values obtained by the conventional tensile tests for both steels and show good agreement to the microstructures of the steel rebars.
9. Theoretical tensile strength values (obtained from mathematical models) are relatively higher compared to the corresponding values of tensile test results.
10. The mathematical models of the yield strength and Rockwell hardness for the TMT steel rebar have shown consistency in determining yield strength from Rockwell hardness with the tensile test results.

11. Theoretical yield strength values calculated from the models were relatively higher compared to yield strength obtained from tensile tests.
12. The yield strength of the TMT steel bars calculated from empirical equations- correlating yield strength and Vickers hardness, shows a little deviation from the test values but are consistent with the microstructures of the steel bars.
13. The regression coefficients for both TS and YS models show consistency with microstructures and carbon equivalent (CE). The data points show good fitness (R^2) on the trendlines.

SCOPES FOR FUTURE WORK

In this study, an initial attempt has been taken to develop mathematical models in term of structure-property relationship for locally produced TMT high strength steel rebars. The main motive behind the work is to easy characterization of the steel rebars to enhance quality products in the industries. But this was a starting for this research work in this field which claims further detail studies in future to advancement. Some future scopes realized from this study was mention below-

1. This study only presented the qualitative investigations on microstructures of the steel rebars. But, to calculate the grain sizes, amount percentage of the constituents, to identify precipitations, more advanced techniques have to be used. So, to observe the microstructures quantitatively, X-ray Diffraction Spectroscopy (XRD), Scanning Electron Microscopy (SEM), Transmission Electron Microscopy (TEM), Software Image Analysis, etc. can be performed.
2. A study on the effects of strain hardening coefficients on mathematical correlations of the properties can be carried out.
3. The residual stress due to rolling and quenching can be taken into account.
4. The variations in the regression constants in the mathematical models can be explained and justified.
5. The ratio of tensile to yield strength obtained from the tensile tests may varies by different test parameters. These mostly effective parameters can be accounted by further investigations.
6. General empirical equations based on microstructures have been used to determine yield strength for the steel rebars. A more specific relation between strength and Vickers hardness can be developed.

REFERENCES AND BIBLIOGRAPHY

[1] Doushanov, D.L., "Control of Pollution in the Iron and Steel Industry", Encyclopedia of Life Support Systems (EOLSS), Vol. VIII, pp.1-5.

[2] Report on "Available and Emerging Technologies for Reducing Greenhouse Gas Emissions from the Iron and Steel Industry" by Office of Air and Radiation, United States Environmental Agency, September 2012.

[3] Kopczynski, C., "High Strength Rebar Expanding Options in Concrete Towers", Structure Magazine, vol.31, pp.1-2, 2008.

[4] Jha, G., Singh, A.K., Bandyopadhyay, N. and Mohanty, O.N., "Seismic Resistant Reinforcing Bars", Journal of Practical Failure Analysis, ASM International, vol.5, pp.53-56, 2001.

[5] Fazal, S., Kwok, J. and Salah, O., "Application of High-Strength and Corrosion-Resistant ASTM A1035 Steel Reinforcing Bar in Concrete of High-Rise Construction", The Council on Tall Buildings & Urban Habitat's, 8th World Congress, Dubai, pp.1-6, 2008.

[6] Bari, M.S., "Use of 500 Grade Steel in the Design of Reinforced Concrete Slab", BSRM Seminar, pp.1-19, 2008.

[7] Takashi, M., Kawano, O., Hayashida, T., Okamoto, R. and Taniguchi, H. "High Strength Hot-rolled Steel Sheet for Automobiles", Nippon Steel Technical Report No. 88, pp.1-12 2003.

[8] Beynon, D., Jones, T.B. and Fourlaris, G., "Effect of High Strain Rate Deformation on Microstructure of Trip Steels Tested under Dynamic Tensile Conditions", Materials Science and Technology, Vol.21, No.1, pp.103-112, 2005.

[9] Tomota, Y., Tokuda, H, Adachi, Y., Wakita, M., Minakawa, N., Moriai, A. and Morii, Y., "Tensile Behavior of TRIP-aided Multiphase Steel Studied by In-situ Neutron Diffraction", Vol.52, pp.5737-5745, 2004.

[10] Hulka, K., "The Role of Niobium in Cold Rolled TRIP steel", J. Materials Science Forum, Vol.473, pp.91-102, 2005.

[11] Islam, M.A., "Thermomechanically Treated Advanced Steels for Structural Applications", Proceedings of MARTEC 2010, the International Conference on Marine Technology, 11-12 December, 2010.

[12] Panigrahi, B.K., Srikanth, S. and Sahoo, G., ―Effect of Alloying Elements on Tensile Properties, Microstructure and Corrosion Resistance of Reinforcing Bar Steel", J. Mat. Engg. Perform., ASM International, Vol.18, pp.1102-1108, 2009.

[13] Manoharan, R., Jayabalan, P. and Palanisamy, K., ―Experimental Study on Corrosion Resistance of TMT Bar in Concrete", ICCBT, pp.239-25, 2008.

[14] Prabir C. Basu, Shylamoni P., and Roshan A. D., ―Characterisation of Steel Reinforcement for RC Structures: An Overview and Related Issues" The Indian Concrete Journal, pp- 19-30, January 2004.

[15] http://abulkhairsteel.com/technology.php; Technology, accessed on 2 June 2014.

[16] Golodnikov, A., Macheret, Y., Trindade, A.A., Uryasev, S. and Zrazhevsky, G., ―Statistical Modelling of Composition and Processing Parameters for Alloy Development", Journal of Materials Science and Engineering, vol.13, pp.633-644, 2005.

[17] Gaško, M. and Rosenberg, G., ―Correlation Between Hardness and Tensile Properties in Ultra-high Strength Dual phase Steels", Journal of Materials Engineering, vol.18, pp.155-159, 2011.

[18] George E. Dieter, JR., ―Mechanical Metallurgy" International student edition, McGraw-Hill, New York, pp. 282, 1961.

[19] Metals handbook, 8th ed., Vol. 11, ―Nondestructive inspection and quality control', Materials Park, OH, and American Society for Metals, pp. 425, 1976.

[20] Umemoto, M., Liu, Z.G., Tsuchiya, K., Sugimoto, S., and Bepari, M. M. A., ―Relationship between hardness and tensile properties in various single structured steels", Journal of Material Science and Technology, Vol. 17, pp. 505-511, April 2001.

[21] Chenna Krishna, S., Narendra Kumar Gangwar, Abhay K. Jha, and Bhanu Pant, ―On the Prediction of Strength from Hardness for Copper Alloys", Journal of Materials, Vol. 2013, pp. 1-6.

[22] Takakuwa, Osamu, Kawaragi, Yusuke, and Soyama, Hitoshi, ―Estimation of the Yield Stress of Stainless Steel from the Vickers Hardness Taking Account of the Residual Stress", Journal of Surface Engineered Materials and Advanced Technology, 3, pp. 262-268, October 2013.

[23] Moteff, J., Bhargava, R.K., and McCullough, W.L., ―Correlation of the Hot- Hardness with the Tensile Strength of 304 Stainless Steel to Temperatures of 1200 ^{0}C", Metall. Mater. Trans. A, Vol. 6A, pp. 1101–1104, 1975.

[24] Lai, M.O., and Lim, K. B., –On the prediction of tensile properties from hardness tests," Journal of Materials Science, vol. 26, no. 8, pp. 2031–2036, 1991.

[25] Noor, M.A. and Ahmed, A.U., –Study on Grade 75 and 60 Reinforcement in RC Design", BSRM Seminar, pp.1-12, 2008.

[26] Workshop –Structural Steels for Civil Engineering Applications", held at Bangladesh university of Engineering and Technology, Dhaka, Bangladesh, 21 June, 2013.

[27] Kabir, I.R. and Islam, M.A., –Hardened Case Properties and Tensile Behaviours of TMT Steel Bars", American Journal of Mechanical Engineering, Vol. 2, No. 1, pp. 8-14, 2014.

[28] Degarmo, E. Paul; Black, J T.; Kohser, Ronald A., –*Materials and Processes in Manufacturing* –, 9th ed., Wiley, pp. 388, 2003.

[29] http://en.wikipedia.org/wiki/Thermo-mechanical_treatment#cite_ref-1, Thermomechanical processing, accessed on 24 May 2014.

[30] http://www.slideshare.net/ansarrizvi/thermo-mechanical-treatment, Thermo Mechanical Treatment, by Ansar Rizvi, Manager Production at Amreli Steels Limited on July 29, 2010; accessed 25 May 2014.

[31] http://www.bsrm.com/products_xtreme.php, Product Information, Accessed on 25 May 2014.

[32] Avner Sydney H.; –*Introduction to Physical Metallurgy"*; 2nd ed.; Tata McGraw-Hill; pp.260, 261, 2007-2008.

[33] William D. Callister, Jr. "Materials Science and Engineering, An Introduction",7th ed., John Wiley & Sons, Inc., Strengthening by grain size, pp. 188.

[34] George E. Dieter, JR., –*Mechanical Metallurgy*" International student edition, McGraw-Hill, New York, 1961, pp. 288.

[35] Tabor, D., –A Simple Theory of Static and Dynamic Hardness", Proc. R. Soc. Lond., series A, Vol. 192, pp. 247-274, 1948.

[36] Cahoon, J.R., Broughton, W.H., Kutzak, A.R., –The Determination of Yield Strength from Hardness Measurements", Metallurgical Transactions, Vol. 2, no. 7, pp. 1979-1983, 1971.

[37] Tabor, D., Journal of the Institute of Metals, Vol. 79, pp. 1-18, 1951.

[38] Bain, Edgar C., and Paxton, Harold W., –*Alloying Elements in Steel*", 2nd ed., pp. 225, ASM, 1966.

[39] Tabor, D., –*The Hardness of Metals*", Oxford, Clarendon Press, pp. 102, 195, 1951.

[40] Marcinkowski, M. J., Fisher, R. M., and Szirmae, A., Trans. TMS-AIME, vol. 230, pp. 676-89, 1964.

[41] Speich, G. R., and Warlimont, H., J. Iron Steel Inst., vol. 206, pp. 385-92, 1968.

[42] Cahoon, J.R., "An Improved Equation Relating Hardness to Ultimate Strength", Metall. Trans., Vol. 3, no. 11, pp 3040, 1972.

[43] Pavlina, E. J. and Van Tyne, C. J., "Correlation of Yield strength and Tensile strength with hardness for steels," Journal of Materials Engineering and Performance, vol. 17, no. 6, pp. 888–893, 2008.

[44] Hill, R., Lee, E. H., and Tupper, S. J., Proc. R. Soc. (London), Vol. 188, pp. 273-290, 1947.

[45] Douthwaite, R. M., and Petch, N. J., Acta Meta. Vol. 18, pp. 211—216, 1970.

[46] Slavskii, Yu. I., and Artemev, Yu. G., Zavod. Lab., Vol. 55, pg.88—91, 1989.

[47] http://en.wikipedia.org/wiki/Statistical_model, Statistical model, accessed on 26 May 2014.

[48] http://www.answers.com/topic/statistical-models, Statistical Model, accessed on 26 May 2014.

[49] http://en.wikipedia.org/wiki/Regression_analysis, Regression analysis, accessed on 26 May 2014.

[50] http://en.wikipedia.org/wiki/File:Linear_regression.svg, accessed on 26 May 2014.

[51] http://en.wikipedia.org/wiki/Rule_of_mixtures, Rule of Mixtures, accessed on May 27 2014.

[52] Alger, Mark. S. M., "*Polymer Science Dictionary"* ,2nd ed., Springer Publishing, 1997.

[53] http://www.doitpoms.ac.uk/tlplib/fibre_composites/stiffness.php, "Stiffness of long fibre composites", University of Cambridge, Retrieved 1 January 2013.

[54] Askeland, Donald R.; Fulay, Pradeep P.; Wright, Wendelin J., "*The Science and Engineering of Materials* , "6th ed., Cengage Learning, pp. 653-656, 2010-06-21.

[55] Voigt, W., "Ueber die Beziehung zwischen den beiden Elasticitäts constant en isotroper Körper". Annalen der Physik Vol. 274, pp. 573–587, 1889.

[56] Reuss, A., "Berechnung der Flie ßgrenze von Mischkristallen auf Grund der Plastizitätsbedingung für Einkristalle". ZAMM - Journal of Applied Mathematics and Mechanics / Zeitschrift für Angewandte Mathematik und Mechanik, Vol. 9, pp. 49–58, 1929.

[57] ASTM Hardness Conversion Standard: ASTM E-140.

[58] Lists the approximate relationship of hardness values to corresponding approximate tensile strength values of steels, table 3, ASTM A 370- 68.

[59] Mukherjee, M., Datta, C., and Halder, A., "Prediction of Hardness of the Tempered Martensite Rim of TMT Rebars", Journal of Materials Science and Engineering: A, vol.543, pp.36-43, 2012.

[60] Datta, R., Veeraraghavan, R., and Rohira, K.L., "Weldability Characteristics of Torr and Corrosion-Resistant TMT Bars Using SMAW Process", Journal of Materials Engineering and Performance, ASM International, vol.11, pp.369-375, 2002.

[61] Avner Sydney H.; "*Introduction to Physical Metallurgy"*; 2nd ed.; Tata McGraw-Hill; pp. 255-256, 2007-2008.

[62] Avner Sydney H.; "*Introduction to Physical Metallurgy"*; 2nd ed.; Tata McGraw-Hill; pp. 271-275, 2007-2008.

[63] Leont'ev, B. A., Buzovskii, Yu. N., "Mechanical properties of steel with a Widmanstatten structure" journal of Metal Science and Heat Treatment, Vol. 10, issue 11,pp. 930-932, November 1968.

[64] Radu, Tamara, Constantinescu, Simona, and Vlad, M., "Morphologies of Widmanstätten Structures and Mechanism Formation in Steels", Materials Science Forum, Vol. 636-637, pp. 550-555, 2010.

[65] http://metals.about.com/library/bldef-Widmanstatten-Structure.htm, Widmanstatten Structure, Accessed in 4 June 2014.